Merging Geological, Seismic Reflection and Magnetotelluric Data in the Purcell Anticlinorium, Southeastern British Columbia

F.A. Cook, Salt Spring Imaging, Ltd., Salt Spring Island, BC, saltspringimaging@gmail.com

Keywords: *British Columbia, geophysics, seismic reflection, magnetotelluric, Purcell Anticlinorium, Sullivan deposit*

Geoscience BC Report 2018-09

Table of Contents

Tables

Figures

1.0 Abstract

Application of the seismic reflection profiling technique coupled with geological data in the Purcell anticlinorium of southeastern British Columbia produces images of structural and stratigraphic variations in the subsurface with detail that is not available with any other geophysical method. When these results are subsequently combined with two-dimensional inversions of magnetotelluric data, they provide an important approach to targeting sedimentary hosted massive sulphide deposits as well as shear and vein deposits in the subsurface.

2.0 Introduction

2.1 General

The purpose of this project is to combine results from two distinctly different geophysical tools (seismic reflection profiling and magnetotellurics) with existing geological and geochemical information in an effort to map the subsurface positions of stratigraphically controlled (e.g., sedimentary exhalative, or SedEx deposits) and structurally controlled (e. g., vein, shear) concentrations of metals. The area of the project is the Mesoproterozoic Belt-Purcell basin in southeastern British Columbia (Figure 1).

The basin hosts the (now-closed) Sullivan mine, one of the largest Pb-Zn-Ag deposits in the world. The Sullivan deposit was discovered 125 years ago, in 1892, and is characterized as a type example of SedEx deposits that are stratigraphically controlled massive sulphides. In the Sullivan example, the deposit formed in a second or third order basin enclosed within the much larger regional Belt-Purcell basin.

Exploration throughout the 20th and early 21st century in the Belt-Purcell basin has revealed a number of smaller, often non-economic, deposits that are similar (e.g., SedEx) to the Sullivan. These include the Stemwinder, North Star, Kootenay King, Estella, among others that are at, or very close to, the surface. However, in addition to the stratigraphically controlled deposits, there are a number of veins and vein-like (e.g., shear) deposits that are found scattered throughout the basin. Probably the most well known are the St. Eugene veins (part of the Society Girl – St. Eugene – Aurora – Guindon shear/vein system) and the Vine vein, both of which are near Moyie, British Columbia.

Therefore, in order to investigate the possibility that either Sullivan-style SedEx deposits, St. Eugene style shear-zones, or Vine vein-like deposits may be present in the subsurface but out of the reach of most normal prospecting methods, it is necessary to be able to map three key characteristics of the subsurface: 1) stratigraphic variations, 2) structural variations, and, 3) physical properties, particularly if such properties can be correlated with appropriate geometric (stratigraphic and/or structural) characteristics.

The geophysical technique that is most effective for mapping the stratigraphic and structural characteristics of the subsurface is seismic reflection profiling. Although reflection profiling is rarely used in mineral exploration, SedEx deposits are particularly well suited for application of reflection profiling due to the necessity for mapping the stratigraphy and structure with few *a priori* assumptions or requirements. In other words, unlike virtually all other geophysical tools, seismic reflection profiling provides images of structures and stratigraphy without significant initial assumptions or models.

A second geophysical approach that is commonly used in exploration for metals is a suite of electromagnetic (EM) methods. These can be effective because metals tend to be highly electrically conductive and the various EM methods that are used are sensitive to such conductivity variations. Nevertheless, it is also important to realize that not all massive sulphides are electrically conductive because they may contain large quantities of relatively non-conductive minerals (e.g., sphalerite, ZnS) and/or they may contain metals that are not interconnected to allow electrical current flow. In addition, elevated electrical conductivity does not necessarily correspond to higher concentrations of metals, as materials such as graphite and (saline) water can also be conductive.

Therefore, the basic objective of this project is the following. By combining seismic reflection profiling with inversions of magnetotelluric data, it may be possible to map, in detail, variations of subsurface electrical conductivity, and to correlate the results with the structural and stratigraphic information provided by the seismic cross section with geological mapping. The spatial resolution provided by this approach may be effective for developing targets in the subsurface that are 'beyond the reach' of surface techniques such as geological mapping alone, or combinations of mapping with soil and rock geochemistry and with near-surface geophysics (e.g., VLF, airborne surveys, resistivity surveys, etc).

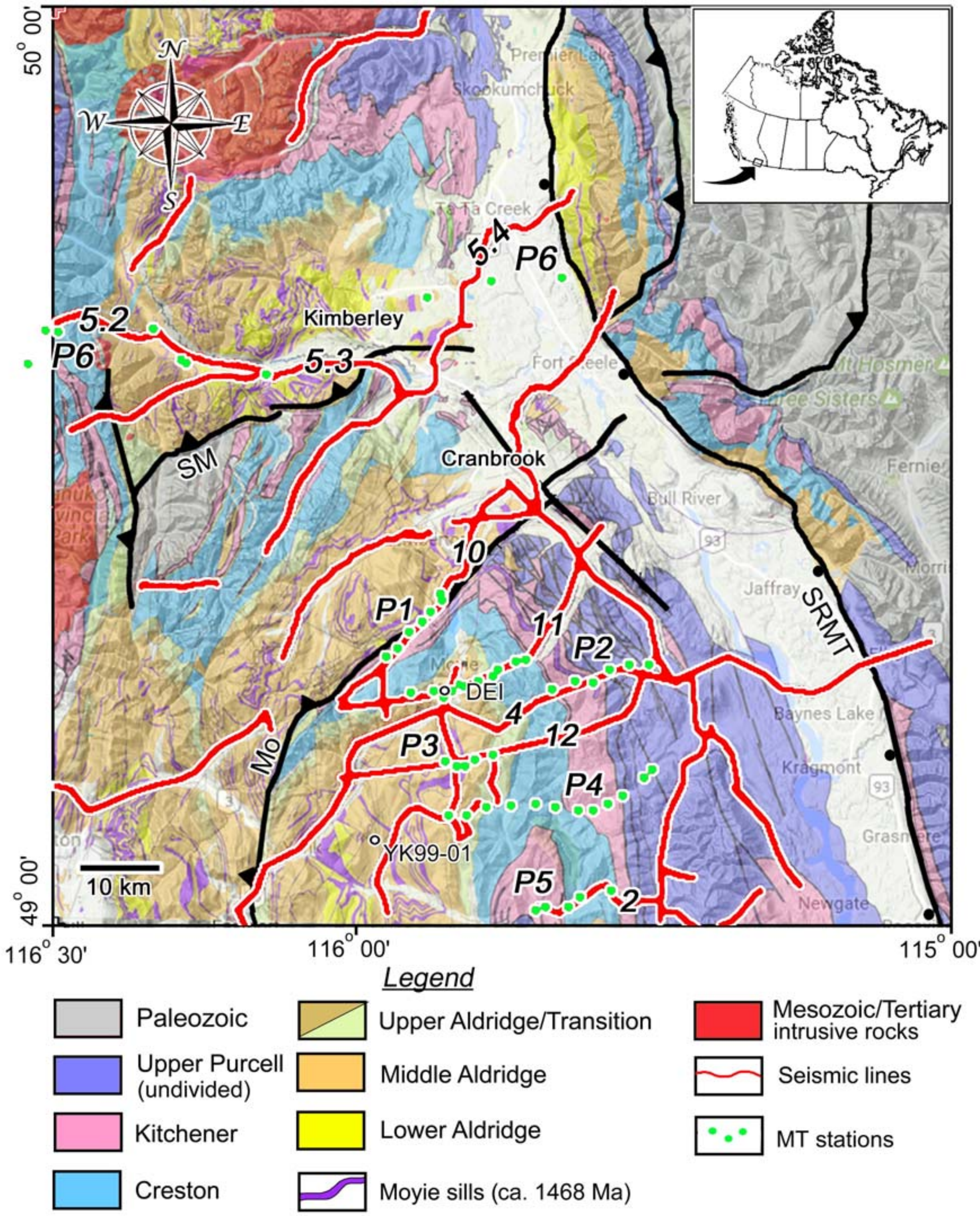

Figure 1. Geological map of the Purcell anticlinorium in southeastern British Columbia. Red lines are the locations of seismic profiles, many of which are used in this study. Seismic line numbers are shown without the 'P' prefix. Thus, the seismic line closest to the U. S. border is line 2 and the northernmost seismic profiles are lines 5.2, 5.3 and 5.4. Numbers with the 'P' prefix are magnetotelluric lines used in this study, with the MT stations shown by the green dots. Abbreviations used are: SM, St. Mary fault; Mo, Moyie fault; SRMT, Southern Rocky Mountain Trench; DEI, Duncan Energy d-8-c drill hole.

2.2 Geological Setting

The geology of the Purcell anticlinorium in Canada and the northwestern United States consists of a thick, generally north-south striking suite of Meso-Proterozoic strata that were deposited in a deep (~20 km or more) basin and that were subsequently uplifted and inverted as the result of eastward-directed contraction during several orogenic episodes including: 1) the late Meso-Proterozoic (East Kootenay orogeny, ca 1.3 Ga), 2) possibly the Neo-Proterozoic (Grenville, ca 1.0 Ga), 3) the Paleozoic (Devonian-Mississippian) contraction, and, 4) finally, the Mesozoic (Cretaceous-Tertiary) Laramide orogeny. The anticlinorium thus developed as a series of stacked anticlines that both strike northward and plunge northward in Canada (Figure 1). Following contraction and uplift, late Tertiary extension along the Southern Rocky Mountain trench fault and related structures (e.g., Flathead fault) resulted in partial dismemberment of the anticlinorium and the development of linear grabens (e.g., Flathead graben, Southern Rocky Mountain Trench).

The focus in this study is the part of the anticlinorium that is exposed in Canada. Here, the deepest exposed rocks are found in the Moyie anticline (Sylvanite anticline in the United States; Harrison, 1972). The Moyie anticline strikes north-northeast and is truncated on the west and northwest by the Moyie fault, a late Mesozoic east-directed oblique thrust fault (Figure 1).

In this area, the stratigraphy of the Meso-Proterozoic rocks consists primarily of the Aldridge Formation (lower, middle and upper), and the overlying Creston Formation, Kitchener Formation and upper Purcell rocks (Figures 1 and 2). Of these strata, by far the thickest are the Aldridge Formation strata, with exposed thicknesses of more than 6 km for the equivalent Prichard Formation in the U. S. (Cressman, 1985). However, interpretations of seismic reflection data in Canada suggest the Aldridge Formation thickness may exceed 10 km in this area (Cook and van der Velden, 1995; van der Velden and Cook, 1996). This would imply that the total thickness of Belt-Purcell rock may approach, or even exceed, 20 km in this area. The Aldridge strata are intruded by gabbroic rocks that typically form regionally extensive sills in the Middle and Lower Aldridge (Moyie sills, ca. 1468 Ga; Lydon, 2007) and, as noted below, are often responsible for the most prominent seismic reflections.

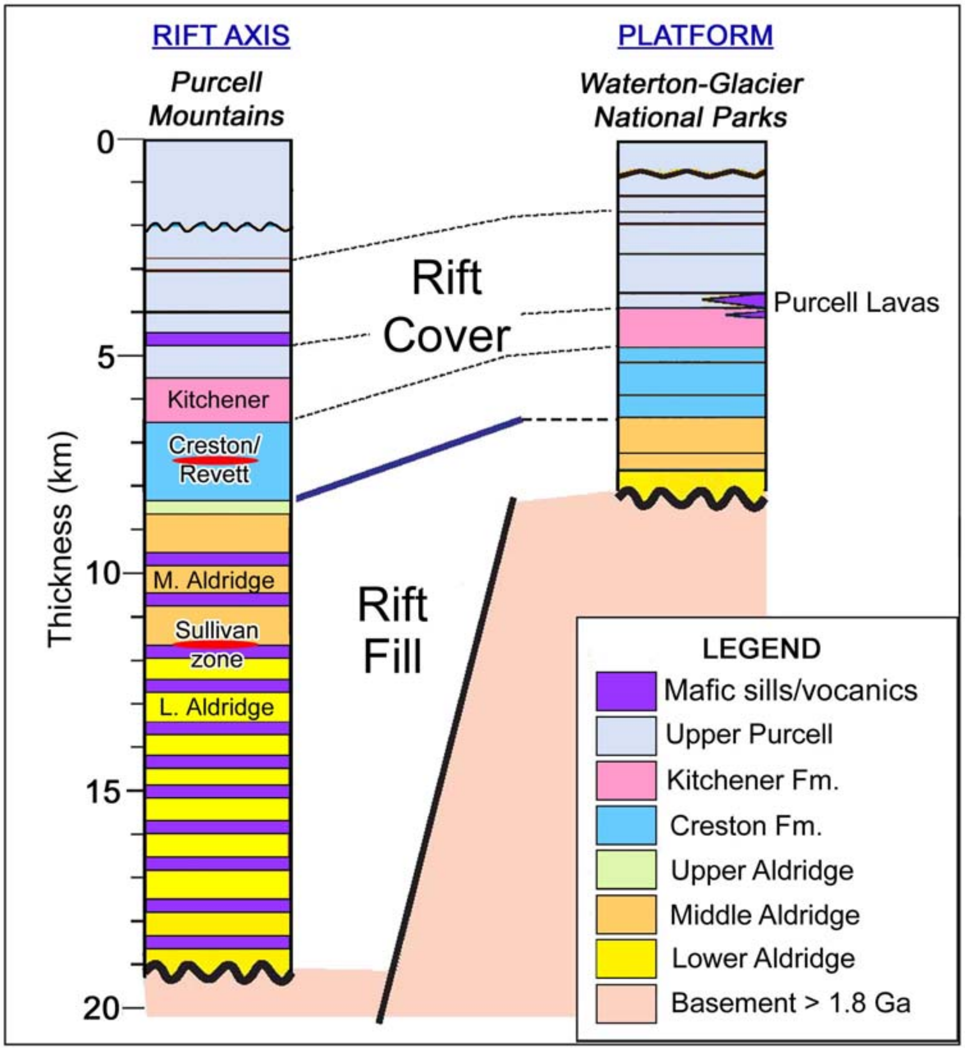

Figure 2. Stratigraphic cross section from the Waterton/Glacier park area on the east to the center of the Purcell anticlinorium in the vicinity of the Moyie anticline on the west (modified from Lydon, 2007). The rocks of greatest interest for this study are the Aldridge, Creston and Kitchener formations. The stratigraphic position of the Sullivan sedex deposit is shown as 'Sullivan zone'.

3.0 Data

3.1 General

The types of geophysical data that are used in this project are seismic reflection profiles recorded for Duncan Energy Corporation in 1984-1985, magnetotelluric data recorded by Phoenix Geophysics for Duncan Energy in 1984-1985, and magnetotelluric data recorded for Lithoprobe in 1991. The Duncan Energy data were acquired as part of a large-scale effort for exploration for hydrocarbons in the area. The idea that the Purcell basin may have potential for hydrocarbons was developed when seismic reflection data in northwestern Montana and southeastern British Columbia produced prominent and regionally extensive reflections (e.g., Cook, 1983); in one view, favourable for hydrocarbon potential, these reflections could be interpreted as resulting from Phanerozoic strata beneath the Proterozoic rocks that are exposed at the surface.

However, the efforts culminated in the drilling of two exploration drill holes, the ARCO #1 Gibbs hole near Libby, Montana (total depth = 5.417 km; Harrison et al. 1985), and the Duncan Oil Moyie d-8-c hole near Moyie, B. C (total depth = 3.477 km; Cook and Jones, 1995). Both of these tests were collared in Meso-Proterozoic Aldridge strata (Prichard in the U. S.) and both of them were terminated in Meso-Proterozoic Aldridge strata; no Phanerozoic rocks were intersected even though a number of prominent and regionally correlatable reflections were encountered. Nevertheless, when combined with detailed geological maps for the Moyie, B. C. area (e.g., Hoy. 1993; Brown et al. 2011), and as discussed below, the Duncan Moyie drill hole provides critical information for delineating the subsurface stratigraphy for southeastern British Columbia and for linking geophysical contrasts (e.g., seismic reflections) to stratigraphic horizons.

3.2 Seismic Reflection Data

Between the U. S. – Canada border at 49° 00’ N. latitude and ~51° 00’ N. latitude (the approximate northern limit of the exposed Belt-Purcell basin strata), Duncan Energy acquired more than 1000 km of seismic reflection data in 1984-1985 (Cook and van der Velden, 1995). The seismic profile locations between 49° 00’ and 50° 00’ are shown as red lines in Figure 1. It is important to recognize that, even though the seismic data were recorded in the mid-1980’s, the data quality is generally good and they still provide information (e.g., stratigraphy, structure) for the subsurface that is not available with any other geophysical method. In addition, in some areas the data can be enhanced with improved filtering and imaging techniques as well as careful iterative applications of standard techniques. Accordingly, the data were initially processed for regional structure (Cook and van der Velden, 1995; van der Velden and Cook, 1996) but were updated and partially reprocessed in 2008-2009 (e.g., Ainsworth, 2009) in an effort to enhance stratigraphic and structural features near the surface; seismic reflection profiling represents a largely underutilized method to target potential for SedEx and related deposits (veins, shear zones) in the subsurface. The seismic lines that were used in this study are included as image files in the appendices as well as lists of the processed CDP (Common Depth Point) locations.

Acquisition parameters for the seismic profiles are shown in Table 1 for the lines in Figure 1 (Cook and van der Velden, 1995). Generally, the lines were recorded with 33.5m station spacing (resulting in nominal 16.75m seismic trace, or CDP, spacing) and most were recorded with the Vibroseis technique. In areas that were not accessible by road, additional lines were recorded with helicopter-portable access and explosive sources (e.g., lines 11p, 12p). Seismic lines that are used in this report are highlighted and underlined in Table 1.

Table 1. Duncan Energy Seismic Profiles and Recording Parameters

Line Numbers	Station Spacing (m)	Source Spacing (m)	Source Type	Sweep Length/ Freqs	Nominal CMP Fold
1.0, 1.1, 1.2, **2.0**, 2.1, 2.2, **4.0**, 5.0, 5.1, **5.2**, **5.3**, **5.4**, 5.5	33.5	67	Vibroseis	12s /14-58Hz	24
2.06, **11.0p**, **12.0p**	33.5	134	Dynamite		20
2.04, **2.05**, **2.07**, 3.1, 3.2, 5.15, 5.25, 5.35, **9.0**, **10.0**, **12.0**. **11.0**, **16.0**, 16.1, 17.0	33.5	100	Vibroseis	12s /14-58Hz	20

Data processing has generally followed the approach listed in Table 2 (Cook and van der Velden, 1995). However, additional processing with variable and more detailed migration velocities and post-stack filtering (steps 11 and 12 in Table 2) has been applied to many of the lines to enhance the near-surface geometry. For most of the data, the elevation datum that was used was 1200m (= 0.0s time on the seismic cross sections) and although the nominal CDP (trace) spacing is 16.75m, this value varies considerably where the lines are not straight.

All processing was applied with an assumption of two-dimensionality (variations are assumed to occur along the lines and in depth. This is necessary because the data were recorded as linear profiles with relatively few (but important) intersections where 3D information may be obtained. This assumption is considered reasonable, however, as the geological structures and stratigraphy often tend to be more-or-less continuous north-south (Figure 1).

Table 2. Processing Parameters for Duncan Energy Seismic Profiles

Parameter	Value (typical, may vary)
1. Demultiplex with gain recovery	
2. Recorrelate with sweep (self-truncating for deep data)	16.0 s of usable data
3. Crooked line geometry	17x500 m bins
4. Time-varying spectral balance	8-48 Hz
5. Amplitude equalization (AGC)	500 ms window
6. Elevation statics	1200m datum; 5500 m/s velocity
7. Normal moveout correction	
8. Stack	nominal 20-24 fold
9. Trace energy balance	8.0-16.0s window
10. Residual statics	1.0-5.0 s window
11. Migration	5000 m/s constant velocity; Reprocessing: variable
12. Coherency filter	variable

3.3 Drill Hole Data

There are numerous drill holes in this area that were completed during normal exploration programs for minerals. However, the deepest and most useful for identifying the origin of important seismic reflections is the Duncan Energy d-8-c drill hole near Moyie, B.C. ('DEI' in Figure 1). This hole was drilled to test the nature of the seismic reflections as well as the coincident elevated conductivity delineated from the magnetotelluric data (e.g., Cook and

Jones, 1995). It was collared in the upper part of the Middle Aldridge Formation and was drilled to 3.477 km depth (Figure 3).

Figure 3 illustrates key information determined from the rocks that were drilled in this hole. On the far left are the resistivity and reflection coefficient logs. The resistivity log is a measure of the formation electrical resistivity in the rocks adjacent to the hole. Three significant observations are relevant here. First, the background resistivity is approximately 1000 Ω-m (= 1 mS/m conductivity) but does show higher values, particularly in some of the sills. Second, some thin zones have relatively low resistivity (near 0.01 Ω-m or 10^5 mS/m conductivity). These commonly occur in the vicinity of the Lower Aldridge–to–Middle Aldridge transition (LMc in Figure 3). The sills (purple in Figure 3) are typically very resistive (>1000 Ω-m).

The reflection coefficient is a measure of how energy is partitioned when it impinges on an interface between rock layers. Some of the energy is reflected back toward the surface and some is transmitted to deeper layers. The reflection coefficient log in Figure 3 was calculated by taking the acoustic impedance (= density x velocity) at each point plus the next deeper point. The difference of the two acoustic impedances divided by the sum of the two acoustic impedances is the reflection coefficient for normal (orthogonal) incidence. Thus, where the reflection coefficient is large (e.g., at about 0.6 and 2.5 km depths), the reflections will be correspondingly large amplitude. At 0.6 km, the large reflection coefficient is due to the contact between relatively low density (~2500 kg/m^3) and low seismic velocity (~5000 m/s) sedimentary rocks above and the higher density (~3000 kg/m^3) and higher seismic velocity (~ 6500 m/s) thick gabbroic sill below. The sill at 0.6 km depth is interpreted as the Sundown sill in the Middle Aldridge Formation. At 2.5 km, the large reflection coefficient is again due to the contact between the sedimentary rocks above and a thick sill below. In this case, the sill is in the Lower Aldridge Formation and may be equivalent to the Bootleg sill near the Sullivan ore body.

The results of the reflection coefficient log were then convolved with a wavelet that has similar characteristics as the Vibroseis wavelet used for the field recording. This technique produces a synthetic (= model) seismic trace that can be correlated with stratigraphic layers (Figures 3 and 4). Once the character of the reflections is established with the drill hole information, the reflection patterns can then be followed to other seismic profiles in the area. A stratigraphic column interpreted from the drilling intersections is shown next to the synthetic seismic trace to show the relationship of the formations and lithologies to seismic reflectivity (Figure 3).

Finally, on the right side of Figure 3, three curves with measured concentrations of Pb, Zn and Cu are shown at the appropriate scale for correlation to the drill hole logs. These geochemical measurements were made on each of the drill cutting samples that were collected during drilling at 3m intervals. Anderson (1987) provided the values of Pb and Zn for the upper part of the hole and Schulze (1988) provided geochemical results for Pb and Zn and added values for Cu to the total depth of the drilling. Two observations are important from these measurements. First, the values of Pb and Zn exhibit elevated values (to 1000 ppm) in the lower part of the Middle Aldridge and upper part of the Lower Aldridge strata. In other words, these elements are anomalous in the vicinity the Lower-Middle Aldridge contact (also known as the LMc). This is the stratigraphic position of the Sullivan deposit.

The second observation from these data that may also be important for interpreting the relationships between conductivity and reflectivity is that Cu values are very low in the Middle Aldridge and upper part of the Lower Aldridge strata (Figure 3) but increase rapidly at about 2.5 km depth. The rocks below 2.5 km consist of thick sills (again, probably equivalent to the Bootleg sills near the Sullivan deposit) that are interlayered with the sedimentary rocks. In addition, however, the region below 2.5 km depth has very few zones with low resistivity, in contrast to the depths between about 1.0 and 2.5 km. Thus, one possible interpretation of the elevated Cu below 2.5 km is that it represents disseminated Cu in the sills, but this is yet to be determined.

Figure 4 illustrates the correlation of the synthetic seismic trace calculated from the drill hole information (Figure 3) spliced into part of adjacent seismic line 11p; the drill hole is located 93m from the closest common depth point (CDP 431) along seismic line 11p. Two splices are shown: one at the location of the DEI drill hole (labeled 'DEI') and a second one about 8 km to the east. The latter helps to illustrate the consistency of the seismic character for the Sundown to Lower Aldridge interval, i.e., there is a three-fold reflection character that includes the following: 1) a prominent Sundown reflection underlain by, 2) a quiet zone (weak or no reflections) near LMc, and 3) prominent Lower Aldridge sill (LAs) reflections. This reflection appearance, or character, is visible throughout much of the Moyie anticline.

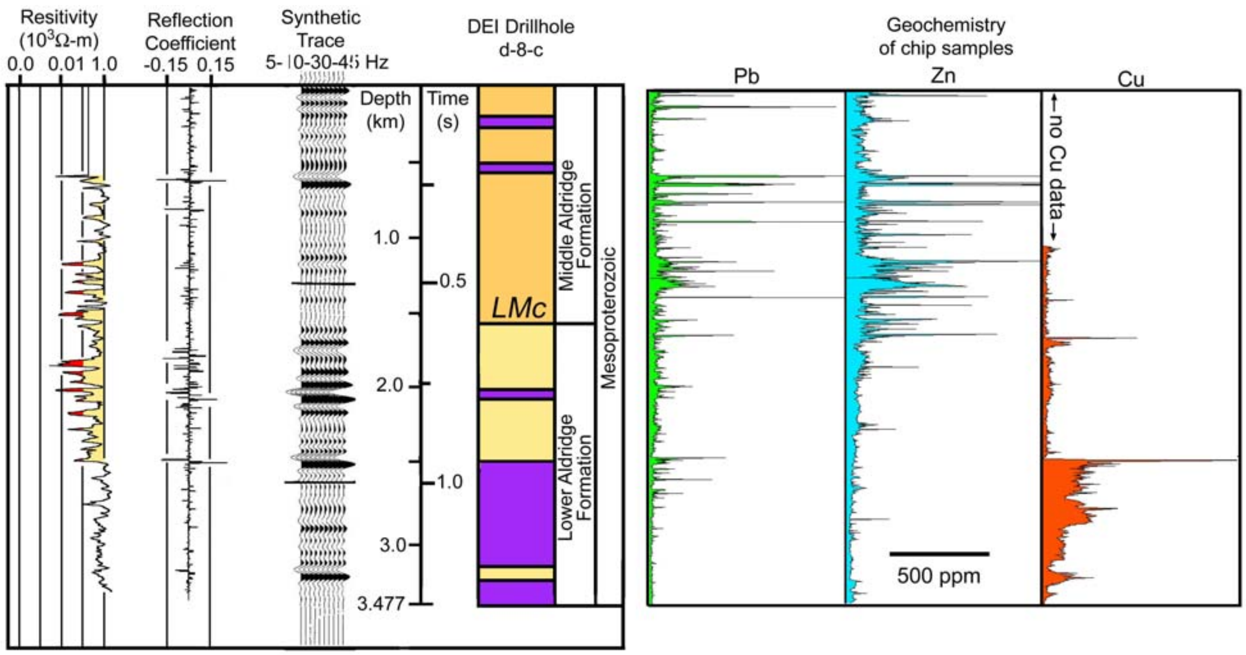

Figure 3. Information derived from the deep Duncan Energy d-8-c drill hole. From left to right these are: 1) the resistivity log; red zones indicate low electrical resistivity (= high conductivity), 2) the reflection coefficient log described in the text, 3) the synthetic trace calculated by convolving the vibroseis wavelet with the reflection coefficient log; 4) the stratigraphic section . The Sundown sill is the second sill (purple) from the top of the section, and, 5) three geochemical logs combined from data presented in Anderson (1987) and Schulze (1988).

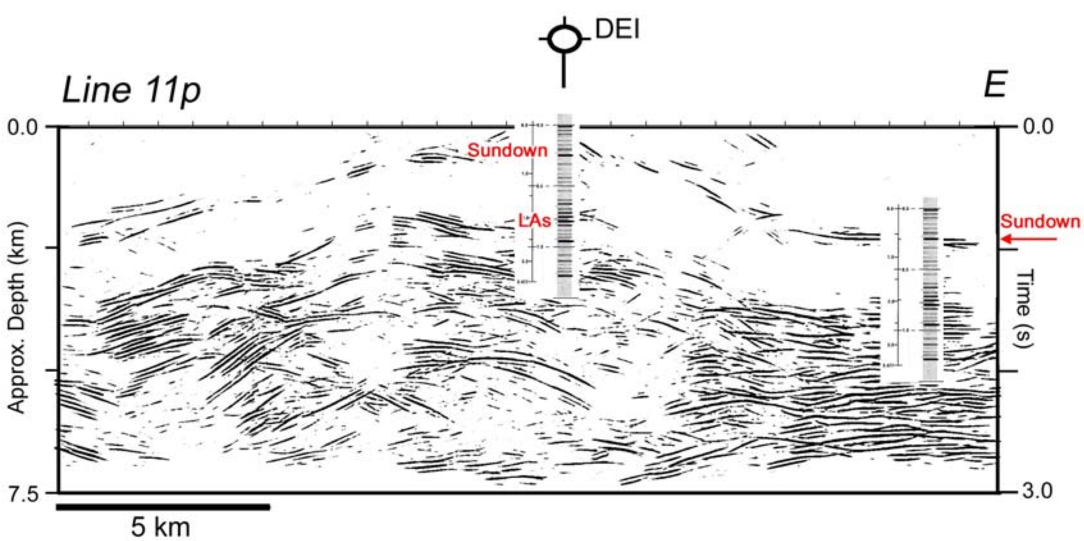

Figure 4. Portion of seismic line 11p with the synthetic seismic trace from the DEI drill hole spliced into the data. Two splices are shown: the one labeled 'DEI' is at the location of the drill hole; the one on the right side of the section projects the drill hole down dip to the east to illustrate the consistent reflection character (sundown reflection – quiet zone near LMc- strong LAs reflections). 'LAs' = lower Aldridge sills (probably partly equivalent to the Bootleg sills).

3.4 Magnetotelluric Data

3.41 Data Sources

The magnetotelluric (MT) data used in this study were recorded in two major programs, one by Phoenix Geophysics for Duncan Energy in 1984-1985 (Gupta and Jones, 1995) and a second, more regional program, by Lithoprobe in 1991 (Jones et al. 1992). The stations recorded for Duncan Energy are represented here as MT lines P1 through P5. Line P6 was recorded by Lithoprobe (Jones et al. 1992).

To assist in clarifying the line locations, as well as the correlations between the seismic profiles and the MT profiles, the following notation is used. For each combined seismic-MT line, the number with the 'P' prefix is the MT line number and each line denoted by a numeral, such as 10 or 5.2 is a seismic line. Thus, line 10-P1 is seismic line 10 and MT line P1. In one case, the line is sufficiently long to include two seismic profiles, so they are both used in the first number (line 4/11-P2).

Table 3. MT Station Information With Associated Seismic Lines

Line Number	No. of Stations	Seismic Line(s)
P1	7	10
P2	22	4/11
P3	5	12
P4	12	12 (projected)
P5	5	2
P6	10	5.2, 5.3, 5.4

3.42 1D vs. 2D inversions

Gupta and Jones (1995) presented 1D inversions for a series of MT lines from near Libby Montana to north of Moyie, BC. In addition, they also presented two examples of early 2D inversions that indicated substantially more lateral variation than is indicated by the 1D inversions. Because 2D inversions allow for variations across strike as well as variations with depth, they can potentially provide much better ability to relate the resistivity/conductivity variation to geological variations along a profile. Variations from profile to profile can provide some information on how resistivity/conductivity varies along strike.

3.43 Geoelectric Strike

A key parameter for applying two-dimensional inversions to the MT data is to determine the orientation of the minimum electric impedance, or the geoelectric strike. Previous authors (Gupta and Jones, 1995; Bedrosian and Box, 2016) have estimated the strike based on induction vectors and phase tensors for the Purcell anticlinorium over the region from nearly 100 km south of the Canada–U. S. border to more than 50 km north of the border. Estimates of geoelectric strike in the U. S. are typically N30W-N50W (330°-310°) which, in turn, coincides well with the general strike of the anticlinorium as delineated by the Moyie-Sylvanite anticline (Bedrosian and Box, 2016; Figure 1).

However, in Canada, the geologic strike of the Moyie anticline changes from a northwesterly strike (N30W-N50W) to a northerly or even northeasterly strike in the area south of Cranbrook (Figure 1). Thus, application of a uniform northwesterly geoelectric strike to the profiles described here may not be appropriate.

The impedance strike is the direction (angle from north) at which the impedance tensor needs to be rotated such that impedance is minimized. For example, Figure 5a shows maps of the impedance strike for frequencies of 0.001 Hz, 0.01 Hz, 0.1 Hz, 1 Hz, 10 Hz, and 100 Hz. Contours are in azimuthal degrees. While there is a general north-south trend to the contours, variations are likely due to 3D effects and/or sparsely spaced data points.

Hence to estimate the strike to be used for the 2D inversion calculations, a series of rose diagrams of the strike directions for each of the lines is shown in Figures 5b. In Figure 5b the diagrams include all of the MT points and all of the frequencies (0.001 Hz, 0.01 Hz, 0.1 Hz, 1 Hz, 10 Hz and 100 Hz), except for 0.001 Hz and 100 Hz frequencies that are not included along lines P2, P4 and part of P5. In Figure 5 the rose diagrams indicate that strike is close to north-south.

Figure 6 shows the same data separated out by MT line. Results for line P1 are at the top and those for line P5 are at the bottom. Although caution should be exercised for lines with few points (e.g., lines P1, P3 and P5), the results indicate that lines P1 and P5 may have slightly different orientation (0°E to 20°E, or 015 to 020) than do lines P2, P3 and P4 (10°W to 00°W, or azimuth 350 to 000). This observation is consistent with the geological structures (Figure 1) which, near line P5, trend northeast (approximately 0 ° to 20 ° E), and near line P1 also trend northeast (approximately 0 °-30 ° E). Near lines P2, P3 and P4, the geologic structures are more-or-less north-south (Figure 1). Thus, the two dimensional inversions were applied with the geoelectric strike for lines P2, P3, P4 and P5 set to North-South (azimuth = 0^o). The geoelectric strike for line P1 is somewhat more difficult to determine due to the few points and variation from approximately 0^o to 30^o E (Figure 6).

To illustrate the sensitivity of some results to the geoelectric strike, Figure 7 shows line P1 inversions for rotations (strike) of 0^o and $+30^o$. Although both show apparent conductors in the upper 6 km or so, their geometries are very different. Because the impedance strike calculated from the data along line P1 tends to indicate the impedance strikes in the western portion of the line are closer to 0^o than the strikes in the eastern part of the line (Figure 4), the inversion for 0^o rotation is used in the comparison to the seismic later in this report.

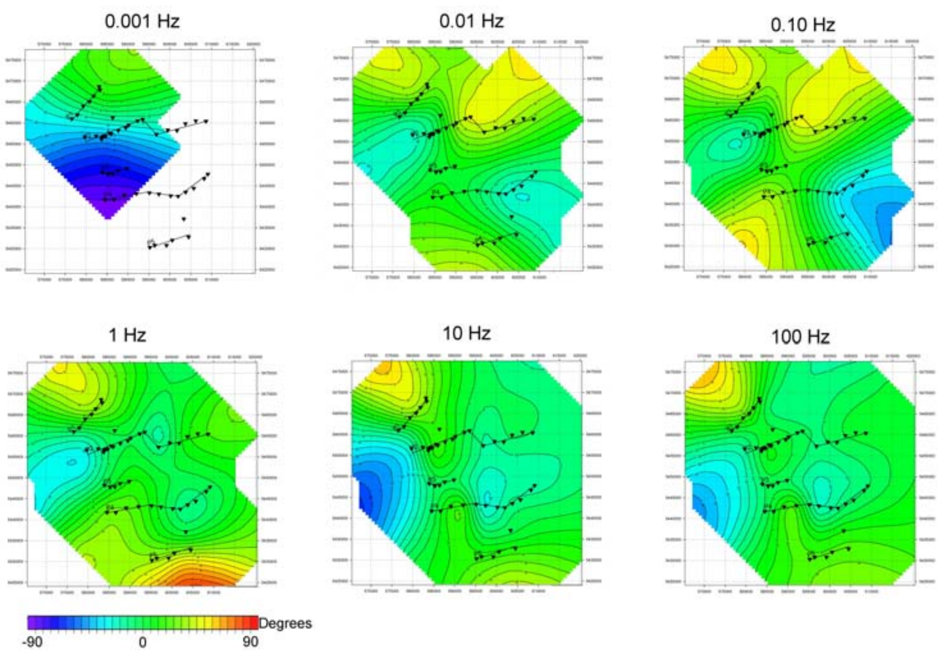

Figure 5a. Maps of the impedance strike for lines P1 (north) through P5 (south) and for different frequencies.

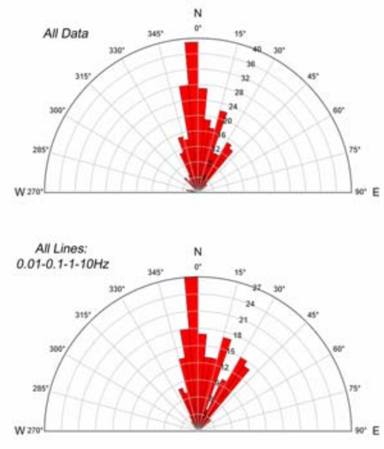

Figure 5b. Rose diagrams for the strike orientation for all lines (P1 through P5) combined and for all six frequencies (top). The lower diagram is a rose diagram of the same data without the 0.001 Hz and 100 Hz frequencies. The diagrams are nearly identical.

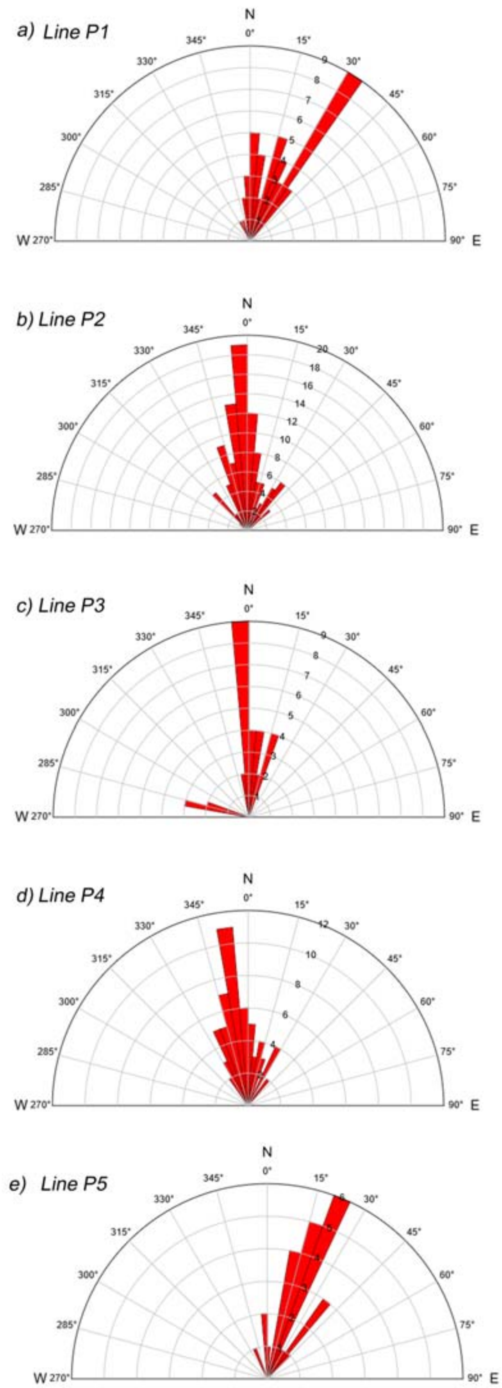

Figure 6. Rose diagrams of the impedance strike for each line, with (a) line P1 at the top and (e) line P5 at the bottom. Diagrams include all six frequency intervals (except for 0.001 Hz along lines P5, part of P4 and part of P2; Figure 5a).

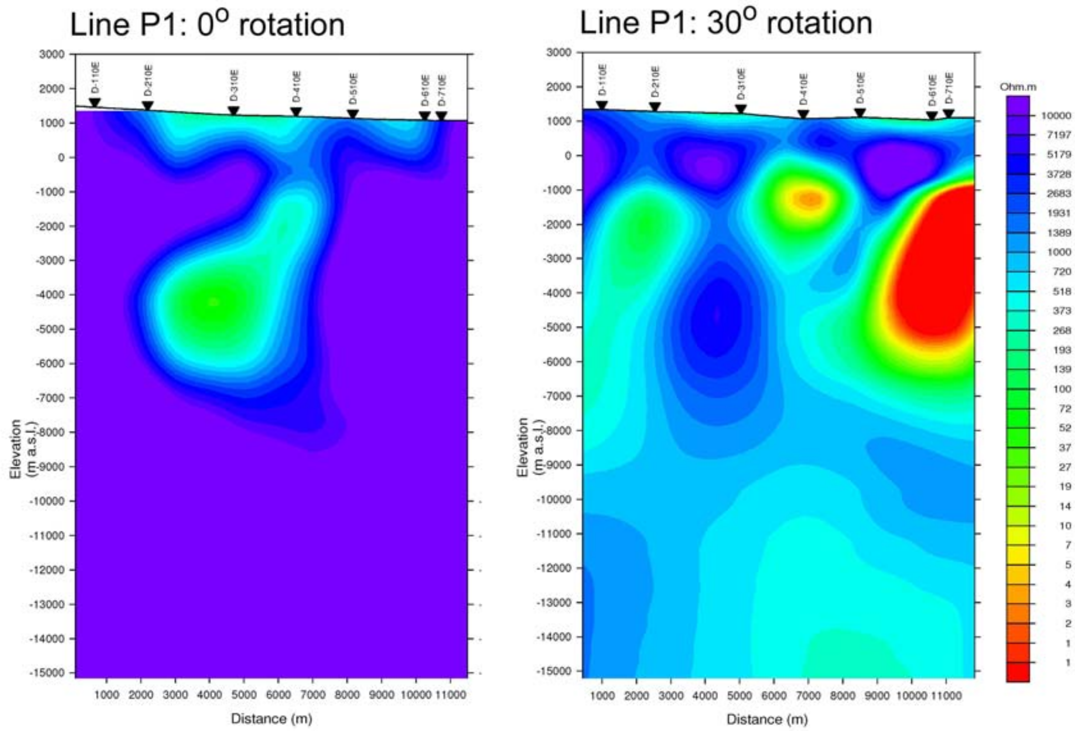

Figure 7. Comparison of inversions for MT Line P1 for (left) 0 degree rotation (North-South strike) and (right), +30 degree rotations (030 strike).

3.43 Inversion Procedure and Ambiguities

Inversions can be done for the transverse electric (TE) mode, the transverse magnetic (TM) mode, or both (e.g., Berdichevsky et al. 1998). For the data used here, the TM mode generally provided the best signal, so the inversions were usually begun with the TM mode, and TE signal was added in during the inversion procedure. Figure 8a shows the typical inversion approach for MT line P4 with the TM mode followed by adding the TE mode signal in progressive decades of frequencies. Alternatively, Figure 8b shows inversion of the same data beginning with the TE mode and adding in the TM mode. Both models produce acceptable statistical fits to the data (not shown here), although the result in Figure 8a produces a slightly better result.

The inversions shown in Figure 8 produce very similar results for the near-surface (+1200m to -6000m) but diverge somewhat for deeper (below -6000m) depths. This appears to be caused by absence of low frequencies in the signal. Nevertheless, both inversions do show a strong conductor below -6000m, albeit with somewhat different geometries.

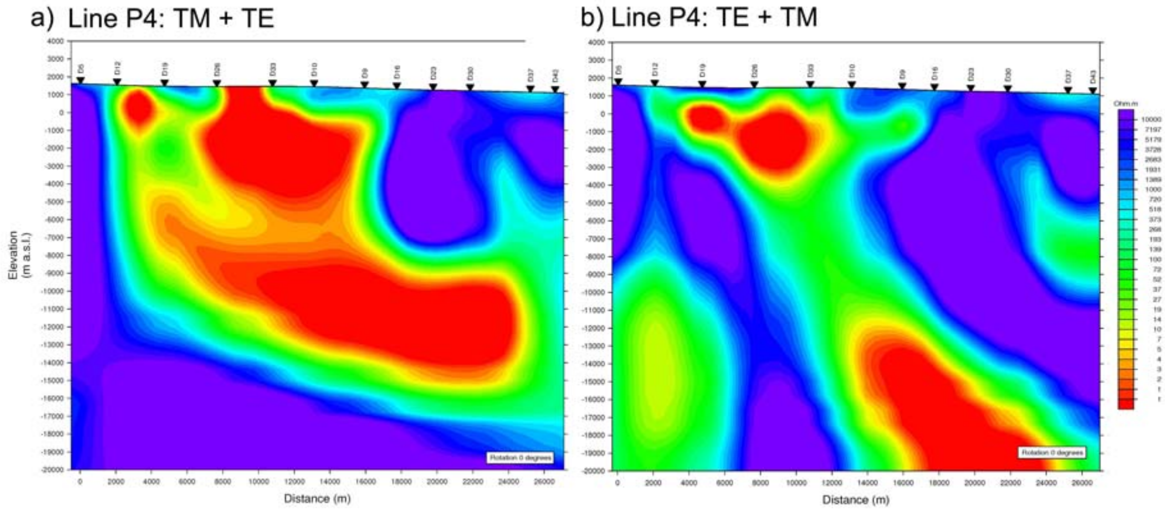

Figure 8. a) Inversion of line P4 starting with the TM mode followed by adding in signal from the TE mode; b) Inversion of line P4 starting with the TE mode followed by adding in signal from the TM mode. The upper 7200 m or so (i.e., elevation from +1200m to -6000m) are very similar, although the deep sections differ, probably due to lack of the low frequencies.

4.0 Results: Moyie Anticline Regional Composite Section

4.1 General

The data across the Moyie anticline consist of a series of four MT profiles and partial profiles that cross the anticline more-or-less at high angles (lines P2 to P5 in Figure 1). Two of these (P3 and P5) are short (5-6 stations) but provide some helpful ancillary information. Line P1 is located on the northwest flank of the Moyie anticline, is subparallel to the Moyie fault, and follows the northeast plunge of the anticline. Line P2 consists of two line segments, one along seismic line 11-11p, and a second along seismic line 4. Following Gupta and Jones (1995), these two segments have been combined into a single long MT profile that crosses most of the northeastern flank of the Moyie anticline. When combined into a single profile, these provide the most complete MT transect of the Moyie anticline. To illustrate the large-scale significance of the results, descriptions of results begin with a regional cross section of the Moyie anticline.

4.2 Regional (Line 4/11–P2) Cross Section of the Moyie Anticline

Figure 9 shows the location of a regional cross section across the Moyie anticline that was constructed by piecing together portions of seismic lines 4 and 11 (Figure 9). The section extends from the Moyie fault on the west to the Rocky Mountain trench on the east. Accordingly, it illustrates a regional view of the subsurface geometry of the anticline and illustrates how the seismic character of the Sundown to LMc to Lower Aldridge sill interval may be correlated over long distances in this part of the Purcell anticlinorium (Figure 10). Moreover, the section provides a perspective of the regional structure that includes the autochthonous North American basement (Canadian Shield) beneath the anticlinorium as well as the deformed Proterozoic strata within the anticlinorium.

During the calculations of the inversions for the MT data, MT line P2 was inverted to significant depth (more than 20 km) and the result is shown in Figure 11. Here the MT profile covers only a portion of the long cross section on the eastern flank of the Moyie anticline. However, it displays a four-fold arrangement of high conductivity zones that effectively summarize the types of features that are visible elsewhere in the area.

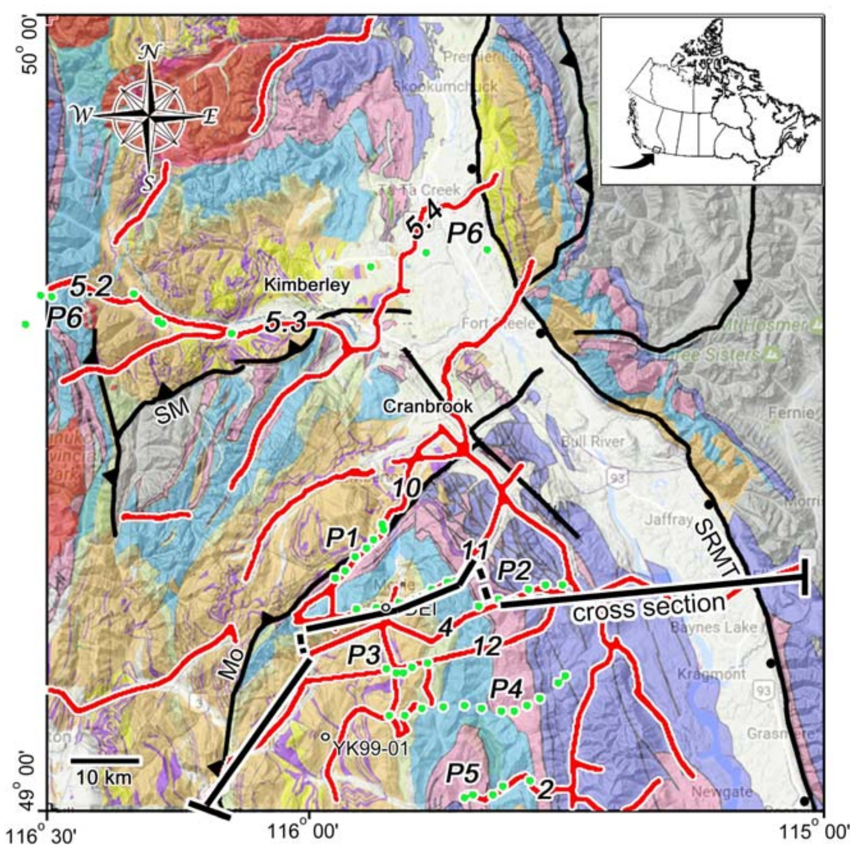

Figure 9. Location of regional cross section across the Moyie anticline in Figures 10 and 11 indicated by the labeled black line.

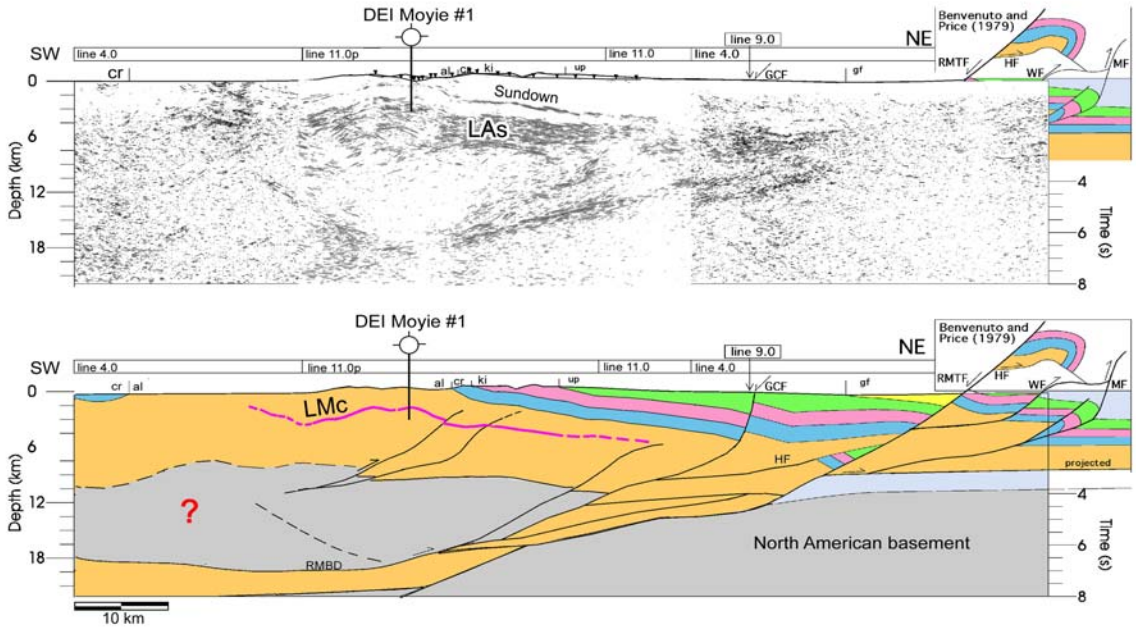

Figure 10. Regional cross section across the Moyie anticline that was constructed by combining portions of seismic lines 4 and 11 (Figure 9). Colours are the same as in Figure 1 with addition of gray for the autochthonous North American basement (= Canadian Shield) rocks. LMC is the approximate position of the Lower-Middle Aldridge contact.

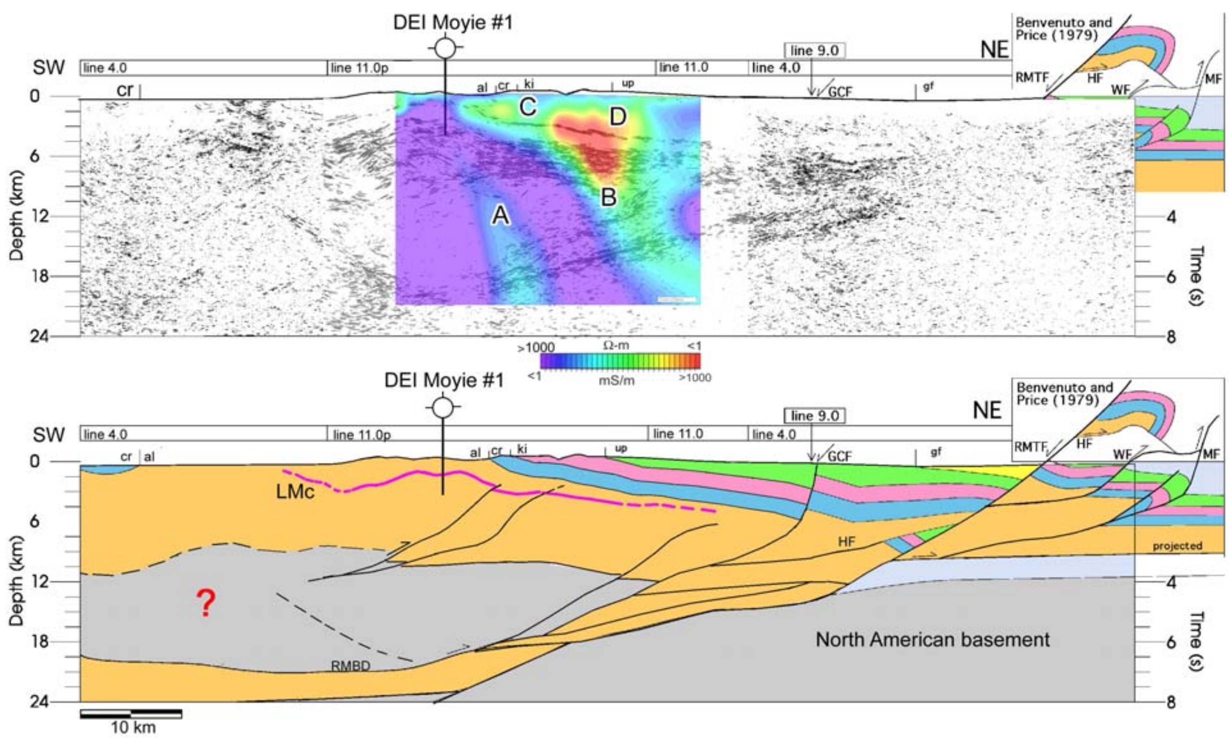

Figure 11. The same profile as in Figure 8 with the MT inversion of line P2 overlain with transparency. Letters A, B, C, and D refer to conductive zones described in the text.

This view provides a considerably more complex geometry of conductors than does the 1D inversion approach presented in Gupta and Jones (1995). By separating different zones of conductivity (four in this case) both vertically and laterally along the section, elevated conductivity can be spatially correlated to stratigraphic and structural features. Four zones are:

1) A deep zone of weakly elevated conductivity (apparently extending to at least 20 km depth) that has a calculated resistivity of ~100 Ohm-m (~10 mS/m conductivity) between about 10 km depth and 20 km depth (‘A’ on Figure 11);
2) A second zone of high conductivity (‘B’ on Figure 11) that is highest at about 6-8 km depth and appears to project downward across the LAs reflections to at least 20 km. Together, conductors A and B have the appearance of ‘conduits’ of conductive material;
3) A third zone of high conductivity (resistivity is about 20 Ohm-m, so conductivity is about 50 mS/m) approximately 4-5 km east of the DEI drill hole (‘C’ on Figure 11), and,
4) A broad zone of elevated conductivity (resistivity is about 1 Ohm-m, so conductivity is about 1000 mS/m) that appears to straddle the strata from above the Sundown sill, into the Lower Aldridge sills (LAs; ‘D’ in Figure 11). The centre of the high conductivity zone is about 15 km east of the DEI drill hole.

4.21 Deep conductor (A)

The deep conductor (A on Figure 11) is centred at about 20 km depth and extends from about 10km to >20 km depth. However, the size is likely to be partly a result of lack of definition due to: a) the relatively low frequencies of the signal at those depths and, b) the relatively wide station spacing. Nevertheless, there does appear to be a weak conductor at or near 18 km depth that projects upward to about 10 km depth.

This is significant because it suggests that there are conduits that may be detected by MT and because the geometry has implications for timing of the conduit formation. According to interpretations by Cook and van der Velden (1995) and van der Velden and Cook (1996), the décollement into which Rocky Mountain thrust faults flatten, projects from the foreland to this location; the rocks below it are likely autochthonous Precambrian basement (labeled ‘North American basement’ in Figures 10 and 11). The interpretation of the rocks immediately above this zone is uncertain. They may be thick Lower Aldridge strata, or they may include one or more slices of the basement as shown in Figures 10 and 11. Thus, if the interpreted conductor A is valid, it is associated either with rocks above the structurally complicated detachment zone (i.e., Aldridge Formation strata or basement), or both and it appears to cross the detachment zone; if so, it may be younger than the basal detachment.

4.22 LAs conductor (B)

Conductor B in Figure 11 appears to be similar to conductor A in that it is steeply dipping and that it appears to cross the detachment zone between the supracrustal rocks above and the North American basement below. As with conductor A, conductor B has the geometry of a conduit-like feature.

4.23 Conductor (C) and conductors above Sundown sill (D)

Conductor C is located in the near-surface east of the DEI drill hole. In zone C, the highest conductivity is located at about 2-km depth and may be associated with the vein/shear deposits of the St. Eugene-Society Girl system.

Conductor D is the strongest conductor on the profile. It appears to straddle the Sundown–to-LAs interval and may even project above the Sundown. Thus, it includes the Lower Aldridge-Middle Aldridge contact (LMc). The LMc is the stratigraphic transition from the Middle Aldridge Formation to the Lower Aldridge Formation (Figure 2); it is significant primarily because it is the stratigraphic position of the Sullivan deposit and has therefore represented a prime exploration target for the last 125 years. Although this stratigraphic horizon will likely continue to be a target for additional sulphide deposits, there is certainly a possibility that additional higher order basins that are not visible at the surface may also be present throughout the basin (e.g., Cook, 2016). Nevertheless, along this profile, the conductivity appears to be elevated along this part of the LMc.

5.0 Results: Moyie Anticline Cross Sections

5.1 General

Five magnetotelluric profiles (P1 through P5) and adjacent seismic profiles constitute a series of cross sections of the Moyie anticline which, by combining the detailed two-dimensional MT inversions with the stratigraphic and structural information from the seismic data, provide clear evidence of how the electrical conductivity varies vertically as well as both across and along strike. In order to illustrate this, each of the sections will be described beginning with the line that is closest to the Canada – U. S. border (Line 2-P5; Figure 1) and then proceeding northward.

5.2 Line 2-P5

Line 2-P5 (seismic line 2, MT line P5) is the southernmost line used in this study. A number of magnetotelluric profiles have been acquired across the anticlinorium in Montana and are described in Gupta and Jones (1995) and more recently by Bedrosian and Box (2016), so they will not be addressed here.

Line 2-P5 crosses only a portion of the Moyie anticline (Figure 1) where a number of thrust faults, collectively known as the Libby thrust belt in Montana, lose displacement and merge with the Moyie anticline to the north (Figure 1). In doing so, these structures appear to have a slightly more northeasterly strike near the Canada-U. S. border than the overall north-northwest strike of the Moyie anticline. This geometric change appears to be reflected in the rose diagram of impedance strike values (Figure 6e) that vary from -30^{o} (330) to +35^{o} (035) with most azimuths around +10^{o} to +25^{o}; Figure 6e). However, MT line P5 does not include values for the lowest frequencies (Figure 5a), so the number of values in constructing Figure 6e is smaller than for other profiles. Nevertheless, inversions were calculated for strike directions of 0^{o} as well as +30^{o} and the difference was very small. Accordingly, the MT inversion for line 2-P5 that is shown here was calculated with an azimuth of 0^{o}.

Figure 12 shows the seismic data from line 2 (Figure 12), an interpretation of the Sundown to Lower Aldridge interval (highlighted by the gray shaded zone in Figure 12b) and the interpreted seismic data overlain with the MT inversion (Figure 12c). Along this profile, the Sundown sill does not produce a prominent reflection as it does farther north (e.g., Figure 10); however, piecemeal reflections at the appropriate distance above the prominent Lower Aldridge sills (LAs) are easily interpreted as the Sundown horizon.

Line 2-P5 crosses the axis of a small anticline that exposes Lower Creston and Upper Aldridge rocks (Figure 1), a geometry that is reflected in the arcuate (convex upward) reflections in the seismic data (Figure 12a). The LAs (Lower Aldridge sills) comprise at least 5 km of stratigraphic section based on the regional seismic profiles through this region (Profile 2 of van der Velden and Cook, 1996).

Merging of the MT inversion with the seismic data (Figure 12c) was accomplished by overlaying the inversion on the seismic between the two endpoints of the MT section. The relatively low resolution of the MT data (i.e., relatively wide station spacing) coupled with, in most areas, the offset of the MT stations from the seismic lines precluded greater detail in the correlations.

In the case of line 2-P5, the MT stations are close to the seismic profile. The inversion indicates that the Lower Aldridge section at this location is highly conductive (Figure 12c). Furthermore, the highly conductive zone appears to have an anticlinal geometry that nearly matches the geometry and spatial position of the anticline defined by the seismic reflections. Although it appears as though the highly conductive zone extends upward almost to the Sundown sill (Middle Aldridge), the few MT stations and relatively wide spacing (1 to 3 km) of the MT stations make this part of the interpretation uncertain.

In any case, although the source(s) of the high conductivity in the Lower Aldridge sill section are unknown, it may be significant that a deep (883m) drill hole (YK99-01 in Figure 1) exhibits a strong increase in copper and nickel composition in the Lower Aldridge, and particularly in the part of the Lower Aldridge that contains the sills about 400-500m below the transition from the Middle Aldridge to the Lower Aldridge (Gal and Weidner, 1999). Accordingly, the highly conductive Lower Aldridge along this profile may indicate significant amounts of copper in this area.

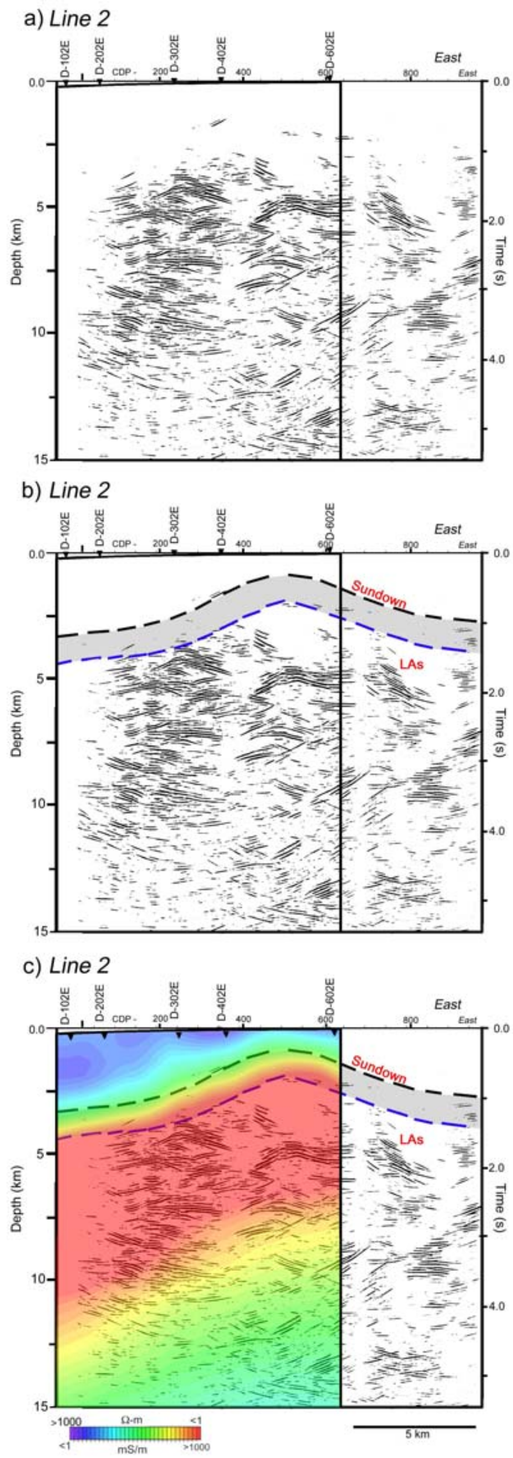

Figure 12. a) Uninterpreted seismic line 2 with the locations of the MT stations indicated; b) b) Interpretation of the Middle Aldridge Sundown (black line) to Lower Aldridge sills (LAs, top indicated with blue line) indicated in gray. The Lower-Middle Aldridge transition (‘Sullivan horizon”) is located within the Sundown-LAs interval; c) Same as (b) with the MT inversion of line P5 overlain. Note that the high conductivity extends to ~12 km depth (about 7-8 km beneath the top of LAs).

5.3 Lines 12-P3 and 12-P4

Magnetotelluric line P4 is located in an area that has no available seismic profiles (Figure 1). Line P3, on the other hand, is located on seismic line 12, although line P3 only has five stations and thus provides conductivity information on a limited portion of the seismic cross section. Figure 13a shows the uninterpreted version of seismic line 12 and Figure 13b is the interpreted section for the Sundown to LAS interval. Figure 13c is the same as Figure 13b with the inversion result from MT line P3 overlain. Although line P3 is only 5 stations, there are two key conductivity anomalies. The most obvious is the strong (red) anomaly near CDP 1300 at about 5-6 km depth. This position corresponds to the locations of two interpreted faults (Figure 13c), but there are too few MT stations to provide much definition of the anomaly.

The second anomaly is located near CDP 1000 at about 1 km depth. It appears to be weaker (lower conductivity) that the anomaly described above, but may be significant when compared to the P4 data set as discussed below.

The results from MT line P4 and its correlation to the seismic geometry are interpreted with two different approaches. First, the Sundown and LAs horizons were mapped on seismic profiles throughout the Moyie anticline to produce map images of the anticline at different stratigraphic levels. In this case, the Sundown and LAs horizons were used. The resulting maps allow the subsurface positions of the Sundown and LAs markers to be estimated in the area with no seismic data. The results from the MT inversion can then be correlated with the mapped stratigraphic intervals. In a second approach, the MT inversions along line P4 can be reasonably projected into seismic line 12 that is 8-10 km north (and along strike) of MT line P4.

The area in which the horizon maps were constructed is shown in Figure 14 and the resulting maps for the Sundown (Figure 15a) and LAs horizons (Figure 15b). Both of these maps clearly show the orientation of the Moyie anticline. Because the UTM coordinates of both the MT stations and the seismic contours are known, the position of the Sundown and LAs surfaces can be merged as shown in Figure 16.

The somewhat more conventional approach of projecting the MT inversion results from line P4 into seismic line 12-12p are shown in Figure 17. As with previous figures, Figures 17a and 17b show the uninterpreted and interpreted (Sundown to LAs), and Figure 17c shows the superimposed MT inversion (see also Figure 8) for line P4 after projection along strike northward to seismic line 12-12p.

The results of merging the MT data with the seismic image indicate that there are four major zones of elevated conductivity (Figures 16 and 17c):

1. A deep conductor (zone 1 on Figures 16 and 17c) that appears to dip eastward from about 5 km below sea level (6.2 km beneath the seismic datum) on the west to about 10-15 km below sea level on the east (although, see discussion of Figure 8; the deep part of the inversion is not well constrained). This elevated conductivity is located in the Lower Aldridge strata beneath the LAs and is thus in a similar position to the elevated conductivity observed on line 2-P5 (Figure 12c). Note that the deep contours may not adequately define the base of conductor 1 due to the relatively wide station intervals.
2. A prominent conductor (zone 2) between MT stations D26 and D9 that appears to extend from 2 to 3 km above the Sundown to the LAs. This conductive zone also straddles the position of the interpreted faults.
3. An appendage (zone 3) from the second conductive zone to the surface between MT stations D26 and D33. This apparent conductor emerges at the surface in the vicinity of significant showings of copper mineralization in the Creston Formation (e.g., Anderson, 2016).
4. An isolated conductor (zone 4) between MT stations D12 and D19 at about 1 km depth.

Although MT line P3 is short, it is also adjacent to part of seismic line 12p, thus providing a close tie of the MT inversion to the seismic line. There are two key observation that are apparent in comparing MT line P3 (Figure 15c) with MT line P4 (Figures 16 and 17c). First, the strong apparent conductivity anomaly on the east side of P3 appears to coincide with the western part of anomaly 2 in Figures 16 and 17c. Second, a less prominent, isolated conductor appears to be present at about 1 km depth on MT line P3 (Figure 15c). This feature coincides with a stronger conductivity anomaly on line P4 (Figures 16 and 17c), thus providing evidence for this anomaly on two separate MT lines.

The prominent high conductivity zone (zone 2 on Figure 16) appears to straddle the Sundown to LAs interval and may extend several km above the Sundown (Figures 16 and 17c). In addition, the high conductivity appears to be limited horizontally (east-west) because the inversion indicates that the high conductivity is spatially associated with faults that displace the Sundown-LAs strata. This observation is strong evidence that these faults were instrumental in allowing fluids/metals migration.

Elevated conductivity appears to project above the Sundown reflector in at least two locations: one above the faults near CDP 1400 (MT stations D26 and D33) on seismic line 12p, and a second farther west near CDP 1000 (MT stations D12 to D19) on seismic line 12 (Figure 17c). Whether these represent conduits is not clear at this time, but their geometry is consistent with such an interpretation. It may be significant that the elevated conductivity at the surface near CDP 1400 coincides with the location of significant showings of metals in the Creston Formation (e.g., Anderson, 2016).

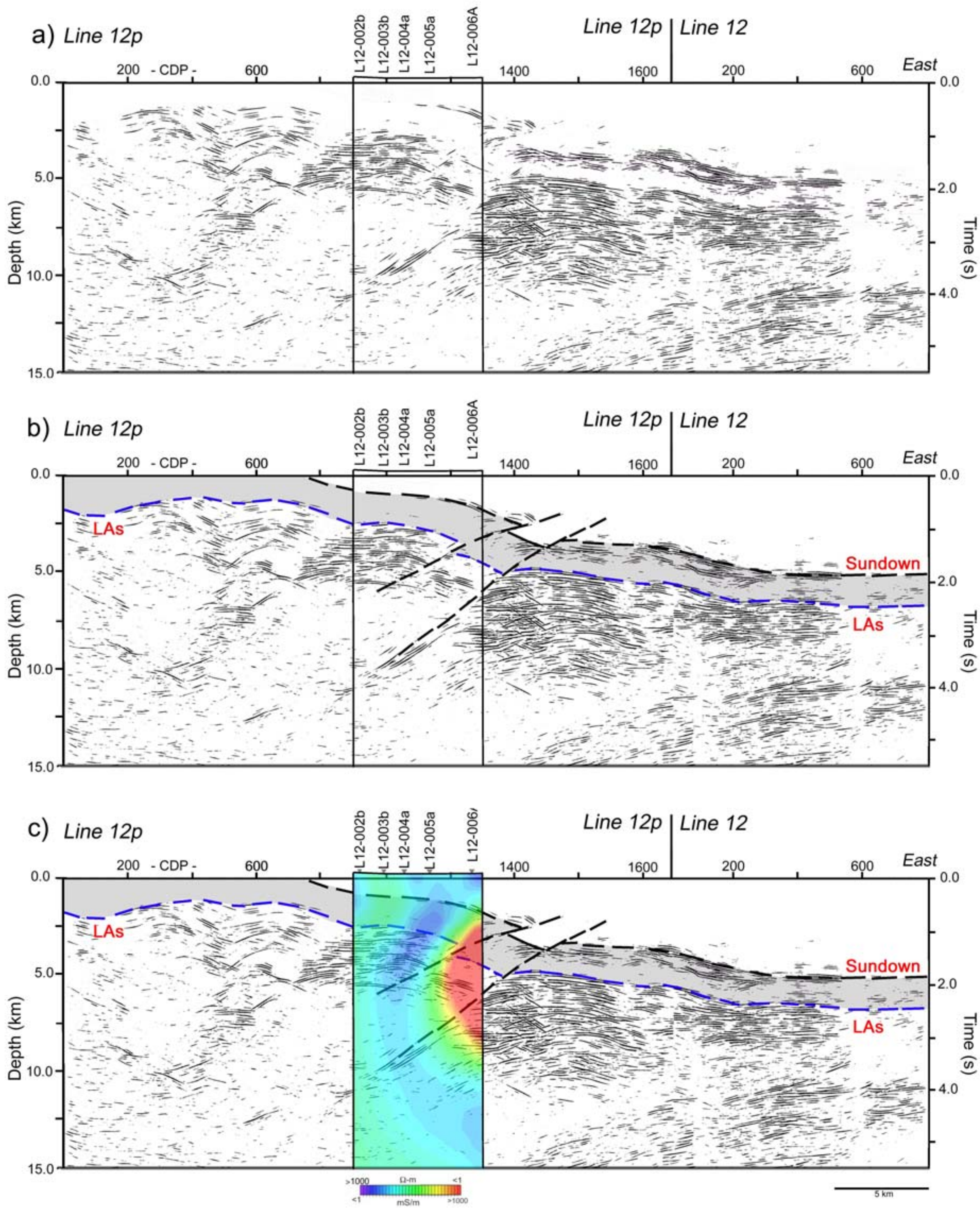

Figure 13. a) Uninterpreted seismic line 12 (12p-12) with the locations of the MT stations ffor MT liner P3 ndicated; b) Interpretation of the Middle Aldridge Sundown (black line) to Lower Aldridge sills (LAs, blue line) interval indicated in gray. The Lower-Middle Aldridge transition ('Sullivan horizon") is located within the Sundown-LAs interval; c) Same as (b) with the MT inversion of line P3 overlain. Note the high conductivity indicated near the interpreted faults.

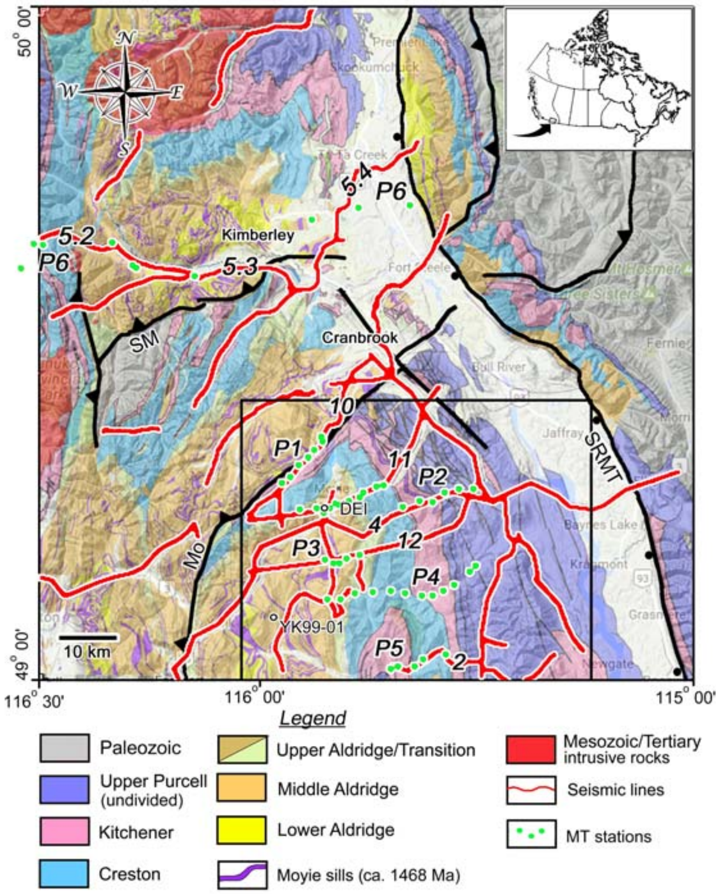

Figure 14. Same map as in Figure 1 showing the area (rectangular outline) within which the maps in Figure 15 were made.

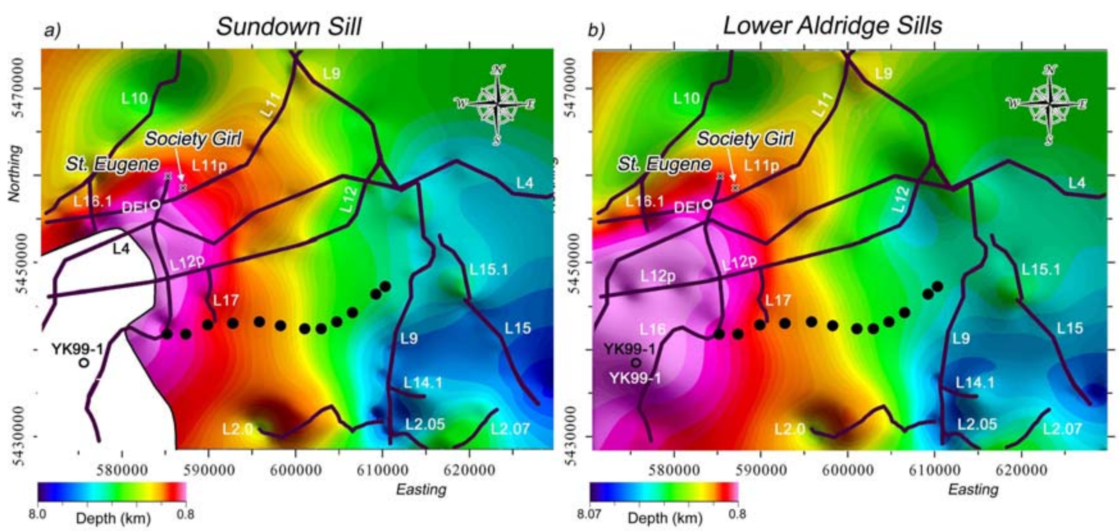

Figure 15. Structure contour maps of the Sundown sill reflection (a) and the LAs boundary (b). Dots are the MT stations along line P4. The white area in the southwest corner of (a) is an area of outcrop (i.e., the Sundown sill is above the surface.

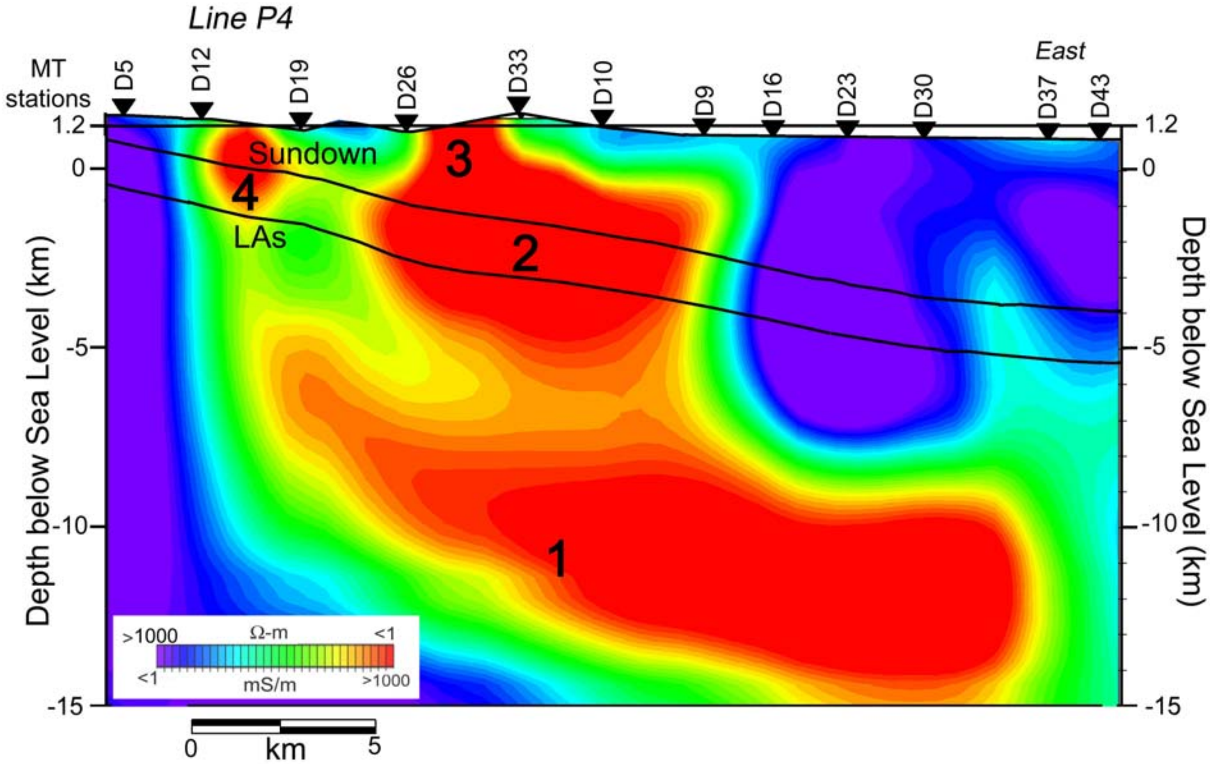

Figure 16. Cross section constructed from the contour maps in Figure 13 to approximate the positions of the Sundown and LAs horizons (dark lines). After conversion to depth and superposition of the MT inversion along line P4 (colour contours), it is apparent that there are four regions of high electrical conductivity: 1) a deep one that dips eastward over most of the section, 2) a prominent zone between 1 and 6 km depth that straddles the LMc, 3) a zone between MT stations D26 and D33 that rises to the surface and, 4) an isolated anomaly at about 1 km depth between MT stations D12 and D19.

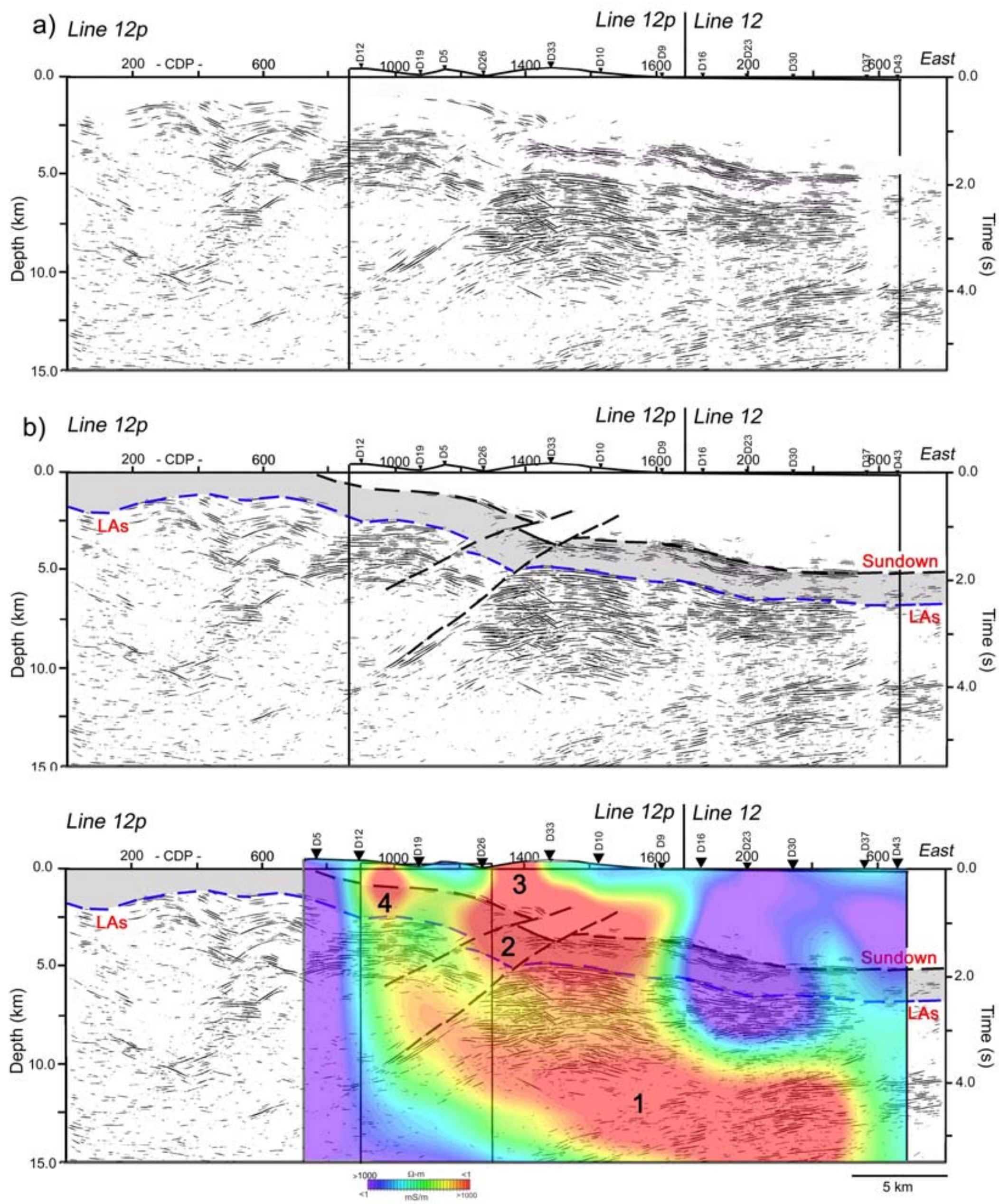

Figure 17. a) Uninterpreted seismic line 12 (12p-12); b) Interpretation of the Middle Aldridge Sundown (black dashed line) to Lower Aldridge sills (LAs, top indicated with blue dashed line) indicated in gray. The Lower-Middle Aldridge transition ('Sullivan horizon") is located within the Sundown-LAs interval; c) Same as (b) with the MT inversion of line P4 projected from the south as indicated in Figure 16. The outline of MT line P3 is also shown for comparison. Note that the highest conductivity (red) projects eastward from the approximate position of the interpreted faults (also, see Figure 13c).

5.4 Lines 11-P2 and 4-P2

MT line P2 is constructed by combining two separate lines that are offset along strike. The western part of line P2 is located on seismic line 11-11p (Figure 1) and is adjacent to the location of the DEI drill hole, thus providing a direct tie between the stratigraphic layers that were intersected in the drill hole and the layers seen on the seismic profile (Figure 4). The eastern part of line P2 is located along seismic line 4 approximately 5 km south of line 11-11p (Figure 1). To account for this in the images, MT line P2 is shown overlain on both seismic line 11-11p and seismic line 4, except that the MT inversion is shown darker where it is overlain on the appropriate seismic profile that includes the MT station locations.

Figure 18a shows the processed but uninterpreted data along seismic line 11-11p and Figure 18b shows the same data with an interpretation of the Sundown-LAs interval. Figure 18c shows the seismic profile with the inversion of MT line P2 overlain. The western portion of the MT inversion is darker because this part of the MT line is on seismic profile 11-11p. The eastern portion of the MT inversion is shown somewhat lighter.

The locations of the conductivity variations (key features are labeled with 'A' through 'D' on Figures 18c and 19c) were discussed previously for the regional cross section and will not be repeated here. However, it is worth noting that the Gupta and Jones (1995) and Cook and Jones (1995) showed 2D inversions along portions of this line and the results are nearly identical to what is shown here (compare Figure 2 of Cook and Jones, 1995 with Figure 18c, particularly in the vicinity of the DEI drill hole).

Figure 19a is an image of the processed but uninterpreted seismic data along part of line 4 and Figure 19b shows the same data with the Sundown to LAs interval interpreted. Figure 19c shows the interpreted section of Figure 19b overlain with the inversion of MT line P2. Because the eastern portion of MT line P2 is on seismic line 4, the inversion results there are shown with darker colours, while the western portion is lighter. As noted previously, the prominent zone of elevated conductivity appears to straddle the Sundown to LAs interval and may even extend downwards to the autochthonous basement. Note also, however, that the widespread elevated conductivity in the Lower Aldridge rocks below LAs is significantly diminished along this profile in comparison to lines 2-P5 and 12-P4. Although the causes of the elevated conductivity in the Lower Aldridge (below LAs) are not yet known for this area, it may be related to the elevated copper observed below LAs in the DEI and YK99-01 drillholes (e.g., Figure 3).

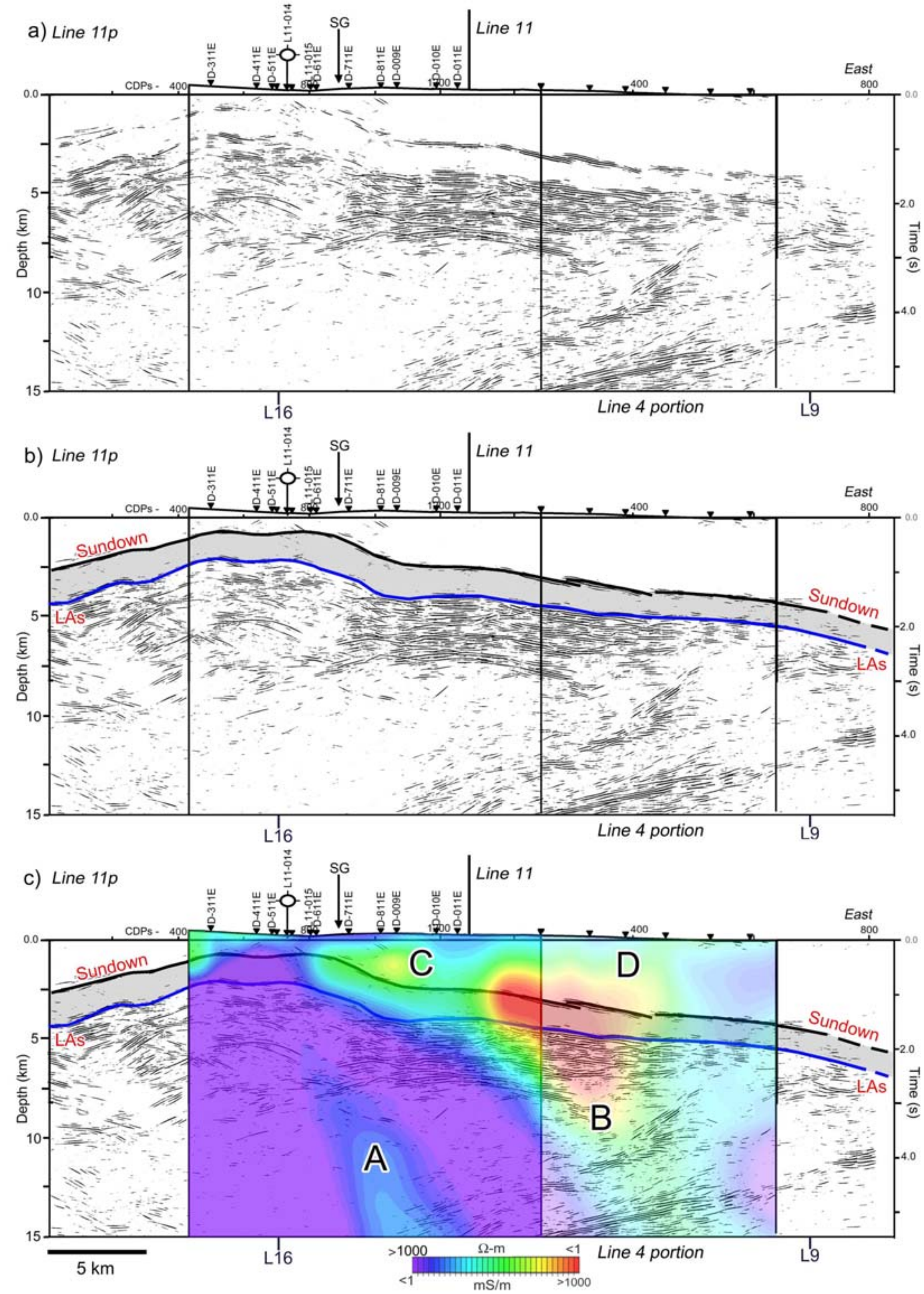

Figure 18. a) Uninterpreted seismic line 11 (combined lines 11p-11); b) Interpretation of the Middle Aldridge Sundown (black line) to Lower Aldridge sills (LAs, top indicated with blue line) indicated in gray. The Lower-Middle Aldridge transition ('Sullivan horizon") is located within the Sundown-LAs interval; c) Same as (b) with the MT inversion of line P2 overlain. Note that the high conductivity (red) is in a similar stratigraphic position as the high conductivity of zone 2 in Figure 17c.

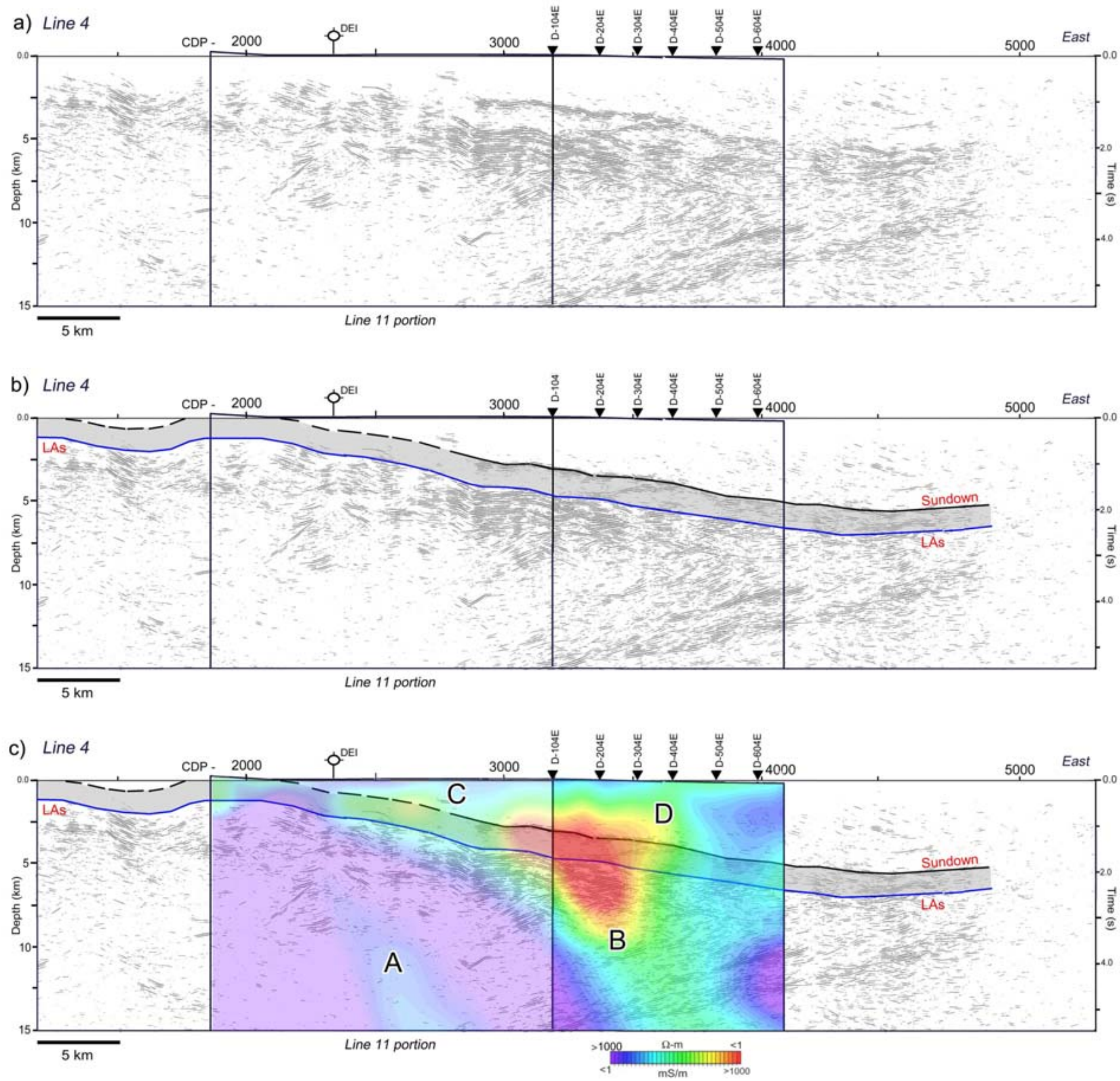

Figure 18. a) Uninterpreted seismic line 4; b) Interpretation of the Middle Aldridge Sundown (black line) to Lower Aldridge sills (LAs, top indicated with blue line) indicated in gray. The Lower-Middle Aldridge transition ('Sullivan horizon") is located within the Sundown-LAs interval; c) Same as (b) with the MT inversion of line P3 overlain. Note that the highest conductivity (red) is in a similar stratigraphic position as the high conductivity along line 12-P4 (Figure 17c).

5.5 Line 10-P1

Line 10-P1 is located on the west flank of the Moyie anticline (Figure 1). At its south end, seismic line 10 is located in the footwall of the Moyie fault and the line orientation is highly oblique to the fault trace. Near the centre of the line, the profile crosses the Moyie fault and remains in the hanging wall of the fault from there to the northeast end of the line (Figure 1). The profile is thus oriented more-or-less parallel to the northeast strike of the structures and strata. This observation is consistent with the rose diagram (Figure 6a) that shows N0E to N30E for the impedance strike of the electrical signals; this contrasts with the dominant North-South strike for lines P2, P3 and P4 (Figure 6), along the eastern flank of the Moyie anticline.

Figure 20a shows the seismic data from seismic line 10 and a geological interpretation focused on the Sundown to Lower Aldridge sills is provided in Figure 20b. The profile exhibits the familiar tripartite seismic character of Sundown – quiet zone (near LMc) – Lower Aldridge sills (LAs). Near CDP 500, the Sundown reflection appears to be disrupted, possibly by a small fault. From CDPs 1400 to 2000, a prominent antiformal structure is visible that is demarcated by a suite of layers between 1.0 and 2.0 s, or about 2.5 – 5.0 km depth. These layers are the Lower Aldridge sills (LAs) in the hangingwall of the Moyie fault and thus represent a duplication of the LAs (see Plate 2d of van der Velden and Cook, 1996) due to the fault. Near CDP 1370, the Vine vein is a deposit located at the surface near the Lower Aldridge – Middle Aldridge stratigraphic transition (LMc).

Two versions of the MT inversion superimposed onto seismic line 10 are shown in Figures 20c and 20d (see also the comparison in Figure 7). The difference between these is that the inversion in Figure 20c was calculated for a geoelectric strike of 0^{o} (North-South), whereas the version in Figure 20d was calculated for a geoelectric strike of $+30^{o}$. These strike values should bracket the values observed in Figure 6a.

In Figure 20c, two conductive zones are visible: 1) a prominent zone near MT stations D210E and D310E at about 5 km depth that appears overlie LMc and is located near a disruption (fault?) in the Sundown reflection, and, 2) a zone in the near surface beneath MT station D210E through D710E (Figure 20c). The first anomaly appears to straddle a wide range of strata from the Lower Aldridge (LAs) to within 2 km of the surface. This would put it (stratigraphically) near the top of the Aldridge Formation or in the Creston Formation. The second conductive zone is confined to the shallow part of the section (0-2 km), although near MT station D410e it may connect to the deeper conductive zone. The wide station spacing prevents delineation of more detail in the near surface.

The version shown in Figure 20d (+30^o rotation) has a very different appearance. In this case, there appear to be three calculated zones of elevated conductivity: one on the west side of the line near the Sundown sill, a second at about 2.5 km depth beneath MT station D410E, and a third on the east side of the MT line in the footwall of the Moyie fault beneath MT stations D610E and D710E. It is not clear which of these strike orientations (0^o or +30^o strike, or an intermediate direction) is more appropriate as the estimates of strike direction from Figure 6a include a range of values. The inversions for the 0^o rotation produced somewhat better fits to the curves; however, the definitive geometry of the conductive zones may have to be determined by additional MT stations, perhaps even a 3D survey. Nevertheless, it appears that the elevated conductivity is confined to the rocks that are stratigraphically at or above the Middle Aldridge Sun down sill.

Additional information on the conductive zone(s) may be obtained by analysing aeromagnetic data near the St. Eugene deposit to project structures into seismic/MT cross section 10-P1. The reason is that the shear zones and veins that were mined in the St. Eugene deposit appear to have a dominant Southeast-Northwest orientation. Hence, mapping of aeromagnetic anomalies may help to project the shear zones northwestward in the subsurface. To accomplish this, data described by Klein (2006) have been reprocessed to enhance geometric information that may be correlated with the structures. To accomplish this task, and because the digital grids were not available, the total magnetic intensity map (Klein, 2006, Plate 3) was digitized and gridded to 50m. The resulting map was then processed by removing an estimate of the Earth's regional magnetic field (International Geomagnetic Reference Field) and then reducing the data to the North Pole. A long wavelength adaptive filter was applied by calculating the upward continuation residual filter for 10 km upward continuation. Finally, the tilt angle was applied to enhance the geometry of the magnetic anomalies. The result is shown in Figure 21. Two clear orientations of linear features are apparent: N30E and N70W; the N70W orientation (white arrows on Figure 21) is the same orientation as the Society Girl – St. Eugene – Aurora – Guindon (SG-SE-Au-Gu) shear zone.

Figure 20 shows this information on a larger scale map that includes the position of seismic line 10 and the stations along MT line P1. To illustrate the potential relationship between the surface information observed near the SG-SE-Au-Gu deposits and line 10-P1 an arrow is drawn through the deposits with an azimuth of N70W to line 10-P1. The position of the projected vein system along line 10-P1, if it exists that far to the northwest, is near MT station D210E, where the Sundown reflection appears to be disrupted and where it has elevated conductivity on both Figure 20c and Figure 20d. Accordingly, the conductive zone near the Sundown reflector at MT station D210E is most easily interpreted as the northwestward continuation of the SG-SE-Au-Gu shear and vein system and it elevated conductivity observed on line 10-P1 indicates that there may be metals present in the subsurface approximately 10 km northwest of the known surface deposits (Figure 22).

Similarly, the processed magnetic data (Figure 21) also indicate that there is a second Southeast structure-Northwest structure (northern arrow in Figure 21) that may project to the position of line 10-P1. As shown on Figure 22, this feature projects approximately to the locations of MT station D410E. Both inversions (Figure 20c and Figure 20d) indicate there is a conductor above the Sundown at about 2.5 km depth. In Figure 20c, this conductor appears to be an upward projection of the conductor near the Sundown, whereas in Figure 20d, the shallow (2.5 km depth) conductor appears to be separate from the deeper conductor.

The distinctly different inversion results for the different orientations suggest that the conductivity structure in this area is complex. In order to improve definition of the nature of the conductivity structure along this profile, it will be necessary to acquire considerably more data, with closer station spacing and perhaps even 3D information. Nevertheless, the spatial correlation of the elevated conductivity and the projections to the northwest of the SE-SG-Au-Gu shear provides an important result that, in addition to stratabound concentrations of metals, it may be possible to target shear and vein systems using this approach of merging seismic images with inversions of magnetotelluric data.

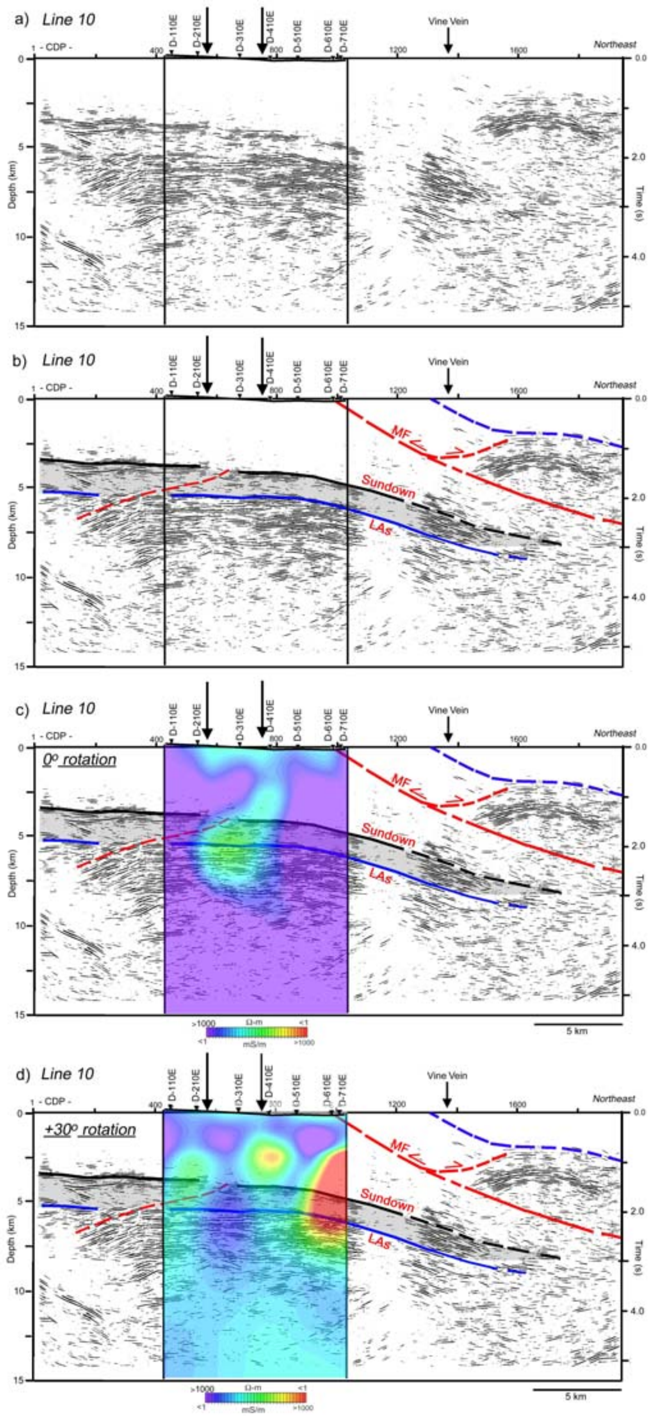

Figure 20. a) Uninterpreted seismic line 10 on the west flank of the Moyie anticline. The arrows near MT stations D210E and D410E are the positions of the projections in Figure 21. b) Interpretation of the Middle Aldridge Sundown (black line) to Lower Aldridge sills (LAs, top indicated with blue line) indicated in gray. The Lower-Middle Aldridge transition ('Sullivan horizon") is located within the Sundown-LAs interval; c) Same as (b) with the MT inversion of line P1 for 0 degree rotation. Note that moderately elevated conductivity appears at the Sundown-LAs interval beneath MT station D210E – D410E, as predicted by projection of the SG-SE-Au-Gu shear/vein system; d) same as (c) for +30 degree rotation.

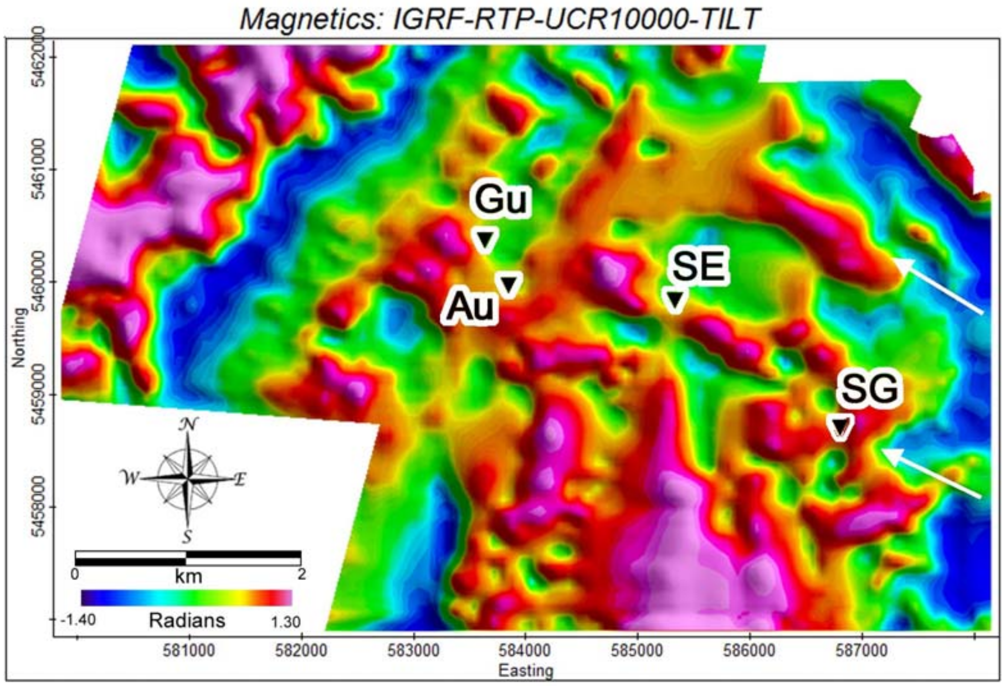

Figure 21. Map of the airborne magnetic anomalies in the vicinity of the St. Eugene deposit (SE). To construct this map, the published total magnetic intensity map in Klein (2006) was digitized and gridded to 50m. Subsequent processing included: 1) removal of the International Geomagnetic reference Field for the dates of the survey, 2) reduction to the North Pole, 3) application of a long-wavelength filter, and the tilt angle. The resulting map displays clear linear anomalies that have an orientation of ~290^o (N70W; white arrows). The Society Girl (SG), St. Eugene (SE), Aurora (Au) and Guindon (Gu) deposits appear to line up along one of the trends.

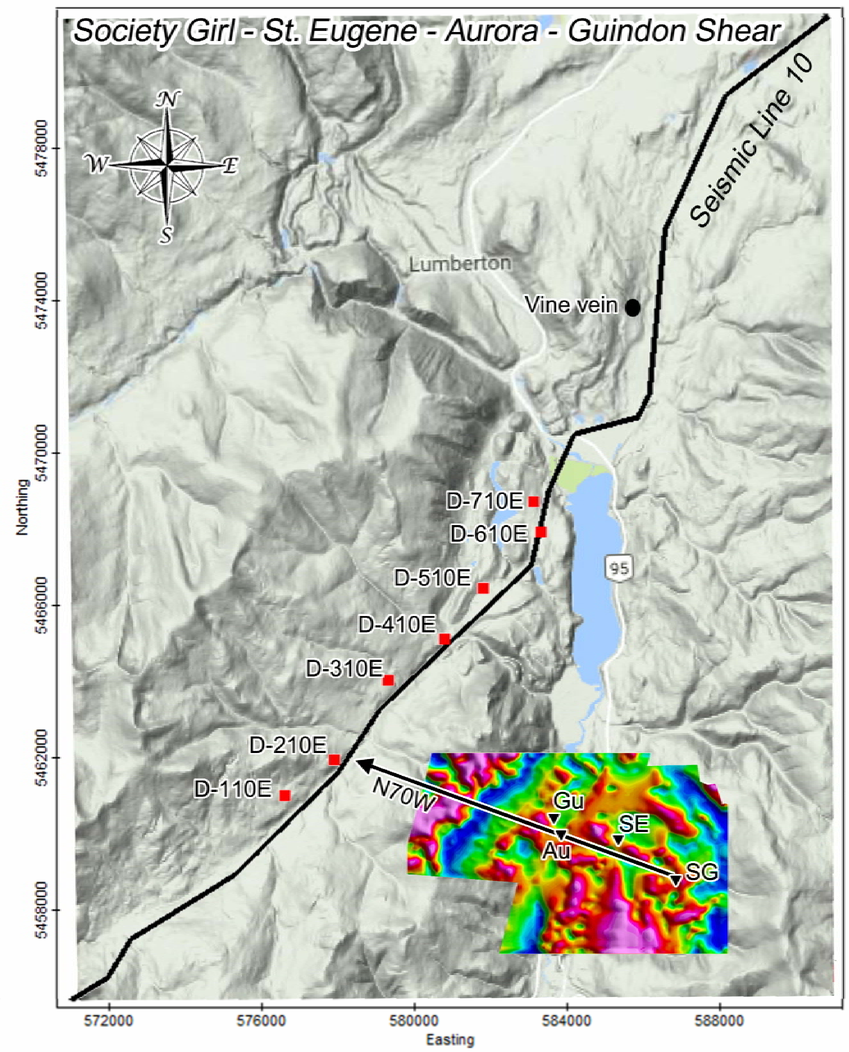

Figure 23. For this map, the map of the magnetic anomalies (tilt angle) is overlain on the topography and the N70W linear vein/shear zone has been projected northwest to the position of the seismic line 10 and the MT line P1 where it appears to intersect near MT station D-210E. Note also that the northern linear anomaly trend would project to between MT stations D-310E and D-410E.

6.0 Results: St. Mary River Area

The purpose of reprocessing the regional profile (MT line P6) north of the Moyie anticline is to address the question of whether the Lower Aldridge sill zone (LAs and below) is electrically conductive throughout the area, or whether its electrical conductivity is restricted in areal extent to localized regions. The station spacing alone line P6 is generally too wide to delineate shallow conductive features with much detail, but the ubiquitous Middle and Lower Aldridge rocks near the surface (upper 15 km or so) along this profile do allow some regional considerations for lateral variations in conductivity in these strata.

Consider line 2-P5 along the U. S. – Canada border (Figure 12). The correlation of the MT results with the seismic results indicates that the Lower Aldridge sills zone (LAs) there is highly conductive. Similar elevated conductivity is visible on the inversions of line P4 to the north (Figures 16 and 17c). A simple extrapolation could then be made that the LAs zone is likely to be conductive elsewhere (e.g., Gupta and Jones, 1995; Bedrosian and Box, 2016). Indeed, Bedrosian and Box (2016) proposed a stratification of electrical conductivity as follows: 1) High resistivity (low conductivity) of Belt/Purcell above the Prichard (= Aldridge) Formation; 2) low to moderate resistivity (moderate to high conductivity) in the bulk of the Prichard (=Aldridge) Formation with local areas of narrow, high conductivity that may correlate with the ‘Sullivan zone’ (Figure 2).

Seismic lines 5.2, 5.3 and 5.4 were recorded along the St. Mary river road west of Kimberley, B. C., then along a series of roads south and east of Marysville (Cook and van der Velden, 1995; Figure 1). MT line P6 consists of 10 stations that were recorded as part of the Lithoprobe program along generally widely spaced stations intervals (Jones et al. 1992; Figure 1). The seven western stations of Line P6 are located on the same road as seismic lines 5.2 and 5.3 and thus tie very well with the seismic data. The eastern three MT stations of line P6 are oriented across seismic line 5.4 and thus any correlation to the seismic geometry there should be undertaken cautiously.

Figure 23 shows the results of combining the MT inversions with the seismic data along this cross section. Two key observations are significant for interpreting this section. First, most of the section to 15 km depth consists of Lower Aldridge (LAs) Formation rocks. Middle Aldridge strata are present at the surface in the footwall of the Hall Lake fault and probably in the footwall of the St. Mary fault (which is crossed twice due to the orientation of the seismic lines). Second, the electrical conductivity structure appears to be highly variable, both along stratigraphic layers as well as across them. In other words, it would be difficult to generalize about the conductivity characteristics of the Lower Aldridge strata along this profile.

This characteristic of variable electrical conductivity both along and across stratigraphic boundaries is one of the themes that derives from the analysis of the results across the Moyie anticline (Figures 12 through 21), and this profile affirms that result farther north.

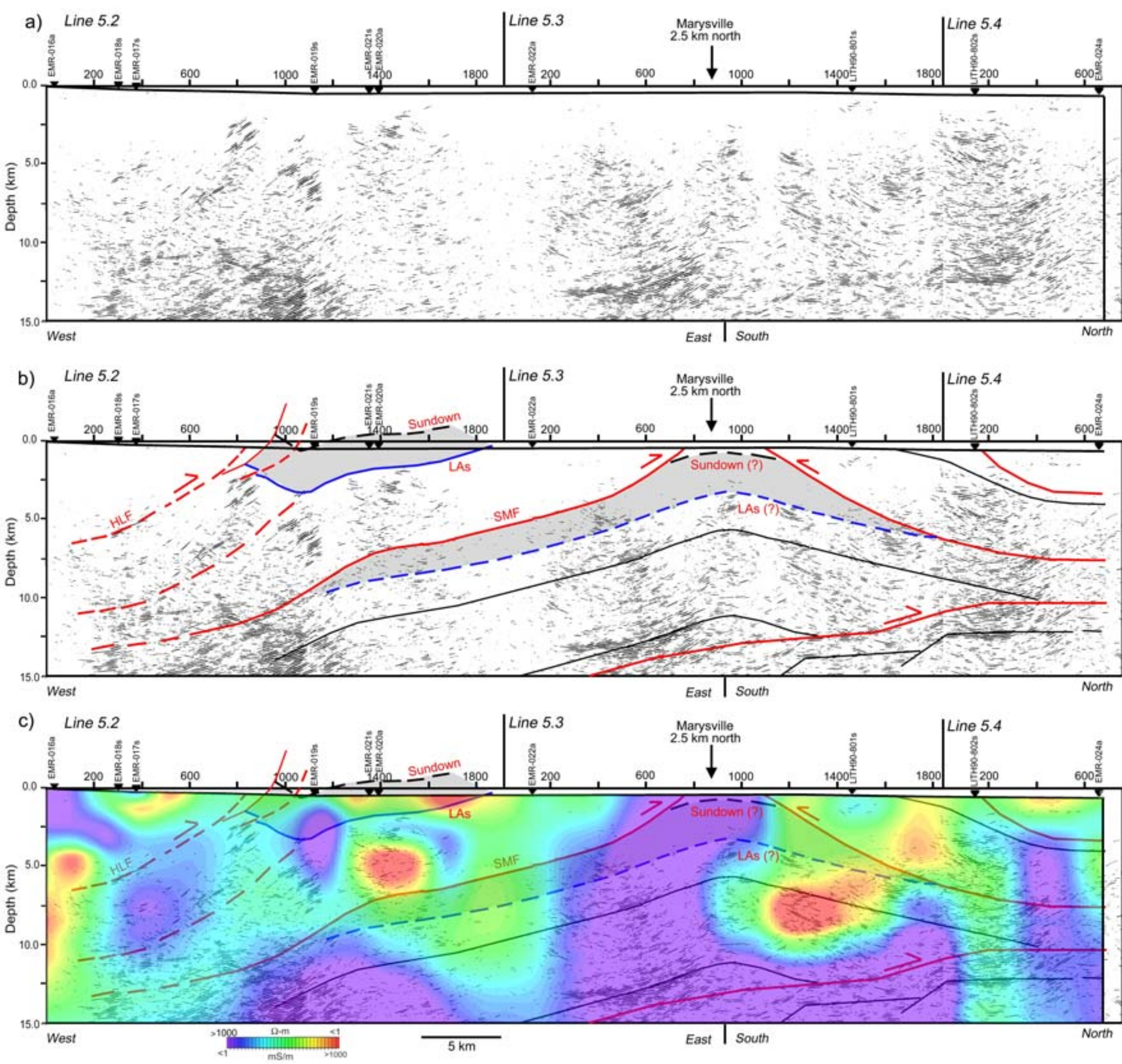

Figure 23. a) Uninterpreted seismic lines 5.2, 5.3 and 5.4 along the St. Mary river road and roads to the east; b) Interpretation of the Middle Aldridge Sundown (black dashed line) to Lower Aldridge sills (LAs, top indicated with blue dashed line) indicated in gray. The Lower-Middle Aldridge transition (‘Sullivan horizon”) is located within the Sundown-LAs interval; c) Same as (b) with the MT inversion. Note the variability of conductivity both within stratigraphic horizons (e.g., Lower Aldridge) as well as across stratigraphic horizons.

7.0 Summary and Conclusions

Application of two-dimensional (2D) inversions to a series of magnetotelluric profiles across parts of the Purcell anticlinorium in southeastern Canada provide new and valuable insight into the relationships between elevated electrical conductivity and stratigraphic and structural variations that are delineated on seismic reflection profiles.

7.1 General Features

By analysing a series of seismic and magnetotelluric profiles at different structural and stratigraphic positions in the Purcell anticlinorium, some results may be generalized for this large region. Following are key observations that have regional significance:

1. Electrical conductivity does not appear to be concentrated in any single stratigraphic interval and varies considerably from location to location within a stratigraphic interval;
2. Electrical conductivity thus appears to vary both across strike, along strike, and with depth for the Proterozoic rocks in the Purcell anticlinorium;
3. Electrical conductivity variations may, in some areas, correlate with shear zones or veins that can be projected from the surface to depth.

7.2 Specific Features

Although the magnetotelluric stations are often more widely spaced than would be ideal for exploration activities, the results are also helpful for focusing on specific variations that can be tied to geological features. These include:

1. Near the U. S. – Canada border (line 2-P5), the Lower Aldridge appears to be highly conductive over a large area. Although it is not clear how far east and west the anomalous conductivity extends, it does appear to be present along the next line to the north (line 12-P4) but appears to have largely disappeared in the lower Aldridge northward to line 4/11-P2;
2. The transition from the Middle Aldridge strata (demarcated by the Sundown sill reflection) to the Lower Aldridge (LAs reflections) includes the 'Sullivan Horizon'. However, it does not appear to be electrically conductive near the U. S. – Canada border (Figure 12c). Along line 12-P4, however, it is highly conductive locally, particularly in the vicinity of fault disruptions (Figure 17c);

3. At a number of locations, the geometry of the conductive zones indicates that elevated conductivity rises to, or near to, the surface. These ‘conduits’ are visible on line 12-P4 (Figure 17c), line 4-P2 (Figure 18c), line 11-P2 (Figure 19c) and, possibly, line 10-P1 (Figure 20c);
4. Along line 10-P1, the calculated conductors appear to coincide with faults and/or shear zones that can be reasonably projected northwestward from the St. Eugene – Society Girl – Aurora – Guindon (SE-SG-Au-Gu) shear zones in Middle Aldridge rocks at the surface to the Middle Aldridge rocks in the subsurface along seismic line 10 (Figures 20 and 22).

In summary, combining these two geophysical techniques (seismic and magnetotelluric) can provide a powerful tool for mapping and targeting stratigraphically and/or structurally controlled zones that may be prospective, but that are hidden from many surface exploration techniques.

8.0 Acknowledgments

This project was funded by Geoscience BC; their support is greatly appreciated. I am also very grateful to Caroline Finateu and Yann Avram at Phoenix Geophysics for spearheading the inversions of the magnetotelluric data and for putting up with, and answering, my many questions. In addition, discussions with Craig Kennedy were helpful for focusing many of the results.

9.0 References

Ainsworth, H. L. (2009): Structure of the Moyie Anticline delineated on a grid of reflection seismic profiles in southeastern British Columbia; MSc thesis, University of Calgary, 82pp.

Anderson, D. (1987): Rock geochemistry of well cuttings from hole Moyie d-8-c on the ML-62, ALD 2, 3, 4, and Sandy 1, 3, 5, 7 claims; BC Ministry of Energy and Mines Assessment report 16681, 18 pp.

Anderson, D. (2016) Assessment Report for geological mapping, Silver Fox Property; BC Ministry of Energy and Mines Assessment report 36022, 27 pp.

Bedrosian, P. A. and Box, S. E. (2016): Highly conductive horizons in the Meso-Proterozoic Belt Basin: Sulfidic early basin strata as key markers of Cordilleran shortening and Eocene extension, *in,* MacLean, J.S., and Sears, J.W., eds., Belt Basin: Window to Mesoproterozoic Earth; Geological Society of America Special Paper 522, p. 1–36, doi:10.1130/2016.2522(12)

Berdichevsky, M. N., Dimitriev, V. I., and Pozdnjakova, E. E. (1998): On two-dimensional interpretation of magnetotelluric soundings; Geophysical Journal International, v. 133, p. 585-606.

Brown, D. A., Macleod, R. F., Wagner, C. L., and Chow, W. (2011): Geology, Moyie Lake, British Columbia; Geological Survey of Canada, Open File 6303, scale: 1:50,000. doi:10.4095/288545.

Cook, F. A. (2016): Integration of geophysical and geological data in the upper Moyie River area: Big Kahuna – STA property; British Columbia Ministry of Energy and Mines, Assessment Report 35883, 45pp.

Cook, F. and Jones, A. (1995): Seismic reflections and electrical conductivity: a case of Holmes' curious dog? Geology, v. 23, p. 141–144

Cook, F. A, and Van der Velden, A. J., (1995): Three dimensional crustal structure of the Purcell anticlinorium in the Cordillera of southwestern Canada; Geological Society of America Bulletin, 107, 642-664.

Cressman, E. R. (1985): The Prichard Formation of the lower part of the Belt Supergroup (Middle Proterozoic), near Plains, Sanders County, Montana; U.S. Geological Survey Bulletin 1553, 64 pp.

Gal, L., and Weidner, S. (1999):1999 geological evaluation of the Yahk property; British Columbia Ministry of Energy and Mines, Assessment Report 26121, 97pp.

Gupta, J., and Jones, A. G. (1995): Electrical conductivity structure of the Purcell anticlinorium in southeast British Columbia and northwest Montana; Canadian Journal of Earth Sciences, v. 32, p. 1564-1583.

Harrison, J. E. (1972): Precambrian Belt basin of northwestern United States: Its geometry, sedimentation and copper occurrences; Geological Society of America Bulletin, v. 83, p. 1215-1240.

Harrison, J. E., Cressman, E. R., and Kleinkopf, M. D. (1985): Regional structure, the Atlantic Richfield-Marathon Oil No. 1 Gibbs borehole, and hydrocarbon resource potential west of the Rocky Mountain trench in northwestern Montana; U. S. Geological Survey Open File report 85-149, 9 pp.

Hoy, T. (1993): Geology of the Purcell Supergroup in the Fernie west-half map area, southeastern British Columbia; British Columbia Ministry of Energy, Mines and Petroleum Resources, Geological Surveys Branch, Bulletin 84, 157 pp.

Jones, A. G. Gough, D. I., Kurtz, R. D., DeLaurier, J. D., Boerner, D. E., Craven, J. A., Ellis, R. G., and McNeice, G. W. (1992): Electromagnetic images of regional structure in the southern Canadian Cordillera; Geophysical Research Letters, v. 19. p. 2373-2376.

Klein, J. (2006): Report on a helicopter-borne Aerotem II/Magnetic survey over the Moyie Lake and Monroe Lake grids, SE British Columbia, Executed by Aeroquest Limited during March 30 – April 7, 2006 on behalf of St. Eugene Mining Corporation, Ltd; British Columbia Ministry of Energy and Mines, Assessment Report 28450, 41pp.

Lydon, J. W. (2010): Tectonic evolution of the Belt-Purcell basin: Implications for the metallogeny of the Purcell anticlinorium; Geological Survey of Canada, open File 6411, 40 pp.

Lydon, J.W. (2008) Mineral deposits of Canada, District Metallogeny, SEDEX – Synopsis of the Belt-Purcell basin; Geological Survey of Canada, http://gsc.nrcan.gc.ca/mindep/metallogeny/sedex/purcell/index_e.php

Schulze, H. C. (1988) Rock geochemistry of well cuttings from well hole Moyie d-8-c on the ML-62, ALD 2, 3, 4 and Sandy 1, 3, 5, 7 claims; BC Ministry of Energy and Mines Assessment report 18128, 34 pp.

Van der Velden, A. J., and Cook, F. A. (1996) Structure and tectonic development of the southern Rocky Mountain trench; Tectonics, 15, 517-544.

10.0 Appendices

Appendix 1 is a brief report provided by Phoenix Geophysics, Ltd. on the inversion procedures. Note that the report states that there was a total of 84 MT sites. However, this number includes several sites east and west on P6 and a few scattered sites that were not included ion the inversions. As noted in Table 3, 61 MT sites were used for this project.

Each of Appendices 2 through 6 has the following:

1. Tiff files of the seismic data for the line. The seismic data are processed through migrations, and are plotted at large scale. All data displayed to 20 seconds two-way travel time, although typically only the upper 5.0 seconds (about 15 km depth) or so were used for the project.
2. UTM coordinates of the CDP (common depth point) locations for each seismic line. The CDP numbers are shown at the top of each seismic profile.
3. UTM coordinates for the MT station locations for each line.
4. UTM coordinates, depth and inversion value for each of the cells in the inversions. Note that the inversions were extended beyond the limits of the MT stations to minimize edge effects in the inversion.

The recorded magnetotelluric data are available from Natural Resources Canada Geophysical Data Centre at:

http://gdr.agg.nrcan.gc.ca/gdrdap/dap/search-eng.php